FOREWORD

This report was prepared by Martin Marietta Denver Aerospace under Contract NAS1-17551. This report covers the results of Task 3. The contract was administered by the Langley Research Center of the National Aeronautics and Space Administration. The Task 3 study was performed from April 1985 to November 1986 and the NASA-LaRC project managers were Mr. U. M. Lovelace and Mr. J. W. Goslee.

CONTENTS

		Page
1.0	INTRODUCTION--BOX TRUSS ANTENNA SYSTEM	1
1.1	Direct Tieback System	3
1.2	Summary	5
2.0	DESIGN AND FABRICATION OF THE REFLECTOR SURFACE	7
2.1	Design of the Reflector Surface	8
2.2	Fabrication of the Reflector Surface	12
2.2.1	Mesh Surface Fabrication	12
2.2.2	Tie System Fabrication	15
2.2.3	Box Truss Standoffs and Tie Cord Adjustments	16
3.0	INTEGRATION OF REFLECTOR AND SURFACE SETTING	21
3.1	Wooden Stands for Mesh Assembly	21
3.2	Installing the Mesh and Tie System onto the Standoffs	22
3.3	AIMS Theodolite Measuring System	26
3.4	Coarse Adjustment of Mesh Surface	26
3.5	Fabrication of Steel Diagonals	27
3.6	Installation onto the Box Truss	28
4.0	VERIFICATION OF REFLECTIVE SURFACE	31
4.1	Photogrammetric Measurements	31
4.2	Best-Fit Analysis	34
4.3	Mesh Pillowing	37
4.4	Surface Area Summary	38
5.0	COMPARISON OF RESULTS WITH ANALYTICAL PREDICTIONS	41
5.1	Mesh Pillowing Equation	41
5.2	Manufacturing Equation	42
6.0	SUMMARY AND RECOMMENDATIONS	43
7.0	REFERENCE	47
	APPENDIX A	A-1 thru A-4
	APPENDIX B	B-1 thru B-9
	APPENDIX C	C-1 thru C-5
	APPENDIX D	D-1 thru D-5

Figure

1	Deployable Box Truss Schematic	1
2	Development of Box Truss, 1980 and 1981	2
3	Box Truss and Direct Tieback Tie System	4
4	4.572-meter Offset-Fed Reflector Geometry	7
5	Tie System Configuration	10
6	Tie System Button Design	12
7	Tricot Knit Weave	13
8	Mesh Fabric	14
9	Reflective Mesh Seam	14
10	Tie System Fabrication Table	15
11	Tieback Cord Adjustment Hardware	17
12	Aluminum Adjustment Fitting	18
13	Attachment Fitting with Adjustment Hardware Installed	19
14	Standoff Assembly	20
15	Wood Stands and Standoffs	21
16	Reflector Surface before to Tie System Tensioning	23
17	Reflector Surface with Tie System Installed and Tensioned	25
18	Diagonal Assembly End Fitting	28
19	Tie Point and Pillowing Target Numbers	32
20	Truss Configuration for Photogrammetric Pictures	33
21	Photogrammetric Camera Positions	34
22	Surface Movements	35
23	Mesh Pillowing	37
24	Redesigned Attachment Fitting	45

Table

1	Error Budget Summary	9
2	Tie Cord Lengths	11
3	Tie Point Location Change	24
4	Baseline Coordinates for Photogrammetric Transformation	33
5	Best-Fit Surface Manipulations	36
6	RMS Surface Error Summary	38
7	Verification of Pillowing Error Equation	41
8	Verification of Manufacturing Error Equation	42

GLOSSARY

cm	Centimeters
D	Reflector Diameter
F	Focal Point
FD	Focal Length over Diameter
GFRP	Graphite Fiber Reinforced Plastic
GHz	Gigahertz
in.	Inch
m	Meters
mm	Millimeter
MT	Manufacturing Tolerance
N	Newtons
NASA	National Aeronautics and Space Administration
OOA	On-Orbit Assembly
rms	Root Mean Square
TS^2	Area Bound by Tie Points
TS_{rad}	Radial Tie Spacing
Z_d	Z Coordinate of Tie Point
Z_p	Z Coordinate of "Best-Fit" Surface

1.0 INTRODUCTION--BOX TRUSS ANTENNA SYSTEM

The basic box truss structure was first designed and used on the On-Orbit Assembly (OOA) program, Contract F04701077-C-0180, for the Air Force (Fig. 1). OOA used the box truss structure to design a planar truss system to support a mesh array. Mesh support posts or standoffs were used to separate the radiating surface from the support structure. The separation provides the volume necessary to stow the mesh and mesh tie-system and to assure that neither the mesh or tie cords will impede the deployment of the box truss. Generally, the standoffs are tubes of similar cross section to the box vertical members and are inserted into the corner fittings. The mesh is attached to the top of the standoffs. In 1979, an IR&D project was performed to determine the adaptability of the box truss to nonplanar shapes, i.e., paraboloidal and spherical reflector systems. The conclusions of the study were as follows:

1) The vertical members on the box truss structure must be vertical rather than perpendicular to the surface to assure step-by-step deployment and stowability.

2) The paraboloid of revolution was the only nonflat surface that can be formed by a box truss structure using equal length standoffs and equal length surface tubes.

3) A spherical reflector can be formed by using a parabolic box truss reflector support structure and varying the mesh standoff heights.

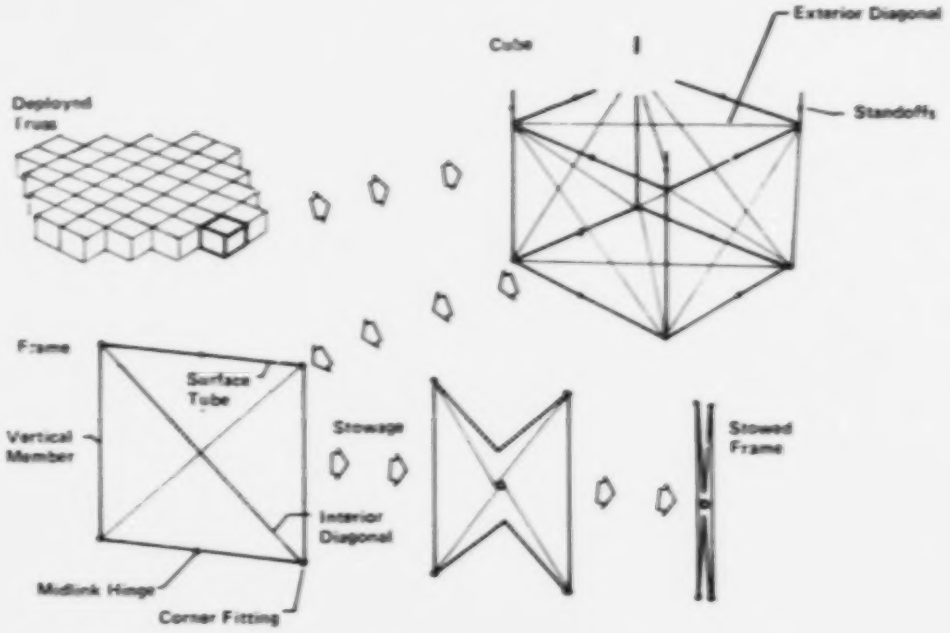

Figure 1 Deployable Box Truss Schematic

From 1981 through 1982, Martin Marietta's IR&D Project D-54D designed and built a single 4.572-m box truss cube using all graphite fiber reinforced plastic (GFRP) components (Fig. 2). Also, included in the D-54D effort was the geometric design of a mesh tie-system, i.e., a web of cords, which would be used to position the mesh into a paraboloid shape.

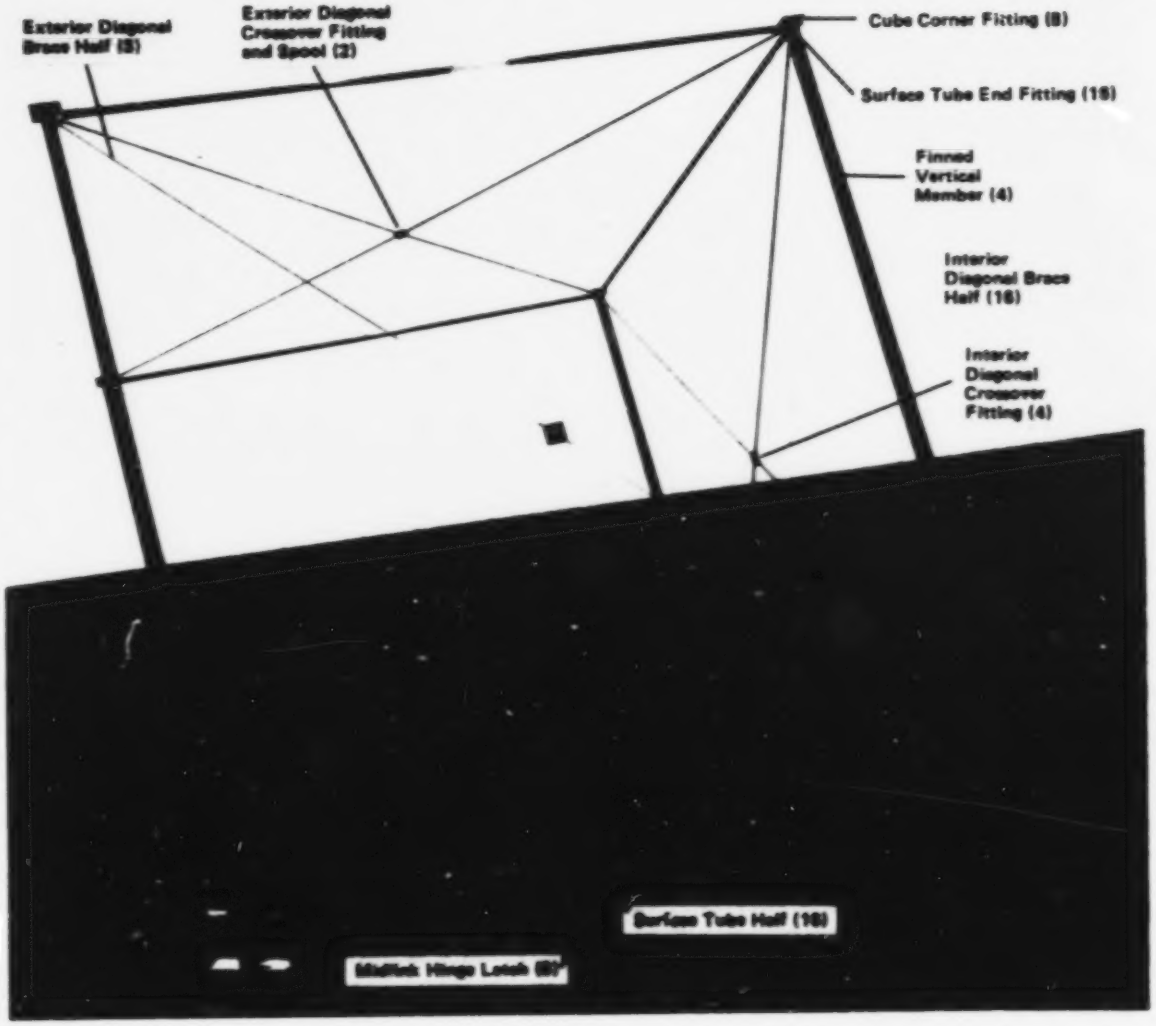
Exterior Diagonal Brace Half (8)
Exterior Diagonal Crossover Fitting and Spool (2)
Cube Corner Fitting (8)
Surface Tube End Fitting (16)
Finned Vertical Member (4)
Interior Diagonal Brace Half (16)
Interior Diagonal Crossover Fitting (4)
Surface Tube Half (16)

Figure 2 Development of Box Truss (1980 and 1981)

To demonstrate the design and integration of a reflective mesh surface to a deployable truss structure, NASA under the Box Truss Analysis and Technology Development Task Contract, Task 3 Integration of Reflector Surface to Box Truss, commissioned Martin Marietta to install a mesh reflector on the 4.572-m box truss cube. The specific features demonstrated include: (1) sewing seams in reflective mesh; (2) mesh stretching to desired preload; (3) installation of surface tie cords; (4) installation of reflective surface on truss; (5) setting of reflective surface; (6) verification of surface shape/accuracy; (7) storage

ORIGINAL PAGE IS
OF POOR QUALITY

and deployment; (8) repeatability of reflector surface; and (9) comparison of surface with predicted shape using analytical methods developed under Task 1--"Mesh Analysis and Control" of this contract.

1.1 DIRECT TIEBACK SYSTEM

From IR&D project studies on various tie system configurations, the direct tieback system has shown analytically to be one of the most stable tie system designs for applying reflective mesh to box truss antennas (Fig. 3). Also, the direct tieback system allows each box section of mesh to be manufactured separately since there are no common tie cords between box sections. This includes the edge catenaries, i.e., each box section would have four-edge catenaries. The mesh would be made continuous by simply sewing the interface together using a whip stitch. If necessary, a separate surface cord with tie backs would be installed at this sewn interface to shape the section of mesh between the two-edge catenaries. Manufacturing each box section of mesh is a desirable design feature considering a single box section may be as large as 15x15 m and having to deploy more than a single box so that the mesh and tie cords could be installed would be cumbersome, if not impractical.

Figure 3 shows that the direct tieback system consists of three types of cords: (1) the surface cross cords that bisect the mesh reflective surface; (2) the surface radial cords that extend radially from the top of the standoffs to the surface cross cords; and (3) the tieback cords that extend from the surface cords to the bottom of the standoffs. The bottom of the standoffs correspond to the location of the corner fittings on the box truss. The tieback cords are used to pull the surface into shape and are tied along each surface cord at a distance defined as the radial tie spacing. Note that the cross cords do not span the entire width of the box section. This is necessary to enable the tie system of each box section to be manufactured separately. Also, this helps to eliminate most of the interaction between the tie systems of adjacent box sections, allowing each tie system of each box to operate independently. Consequently, this produces a more stable reflector surface since local environmental effects such as shadowing of a single box section will not effect the surface of other box sections. Since each tie system can operate independently, analyzing and testing the complete reflective surface can be performed on a per box section basis.

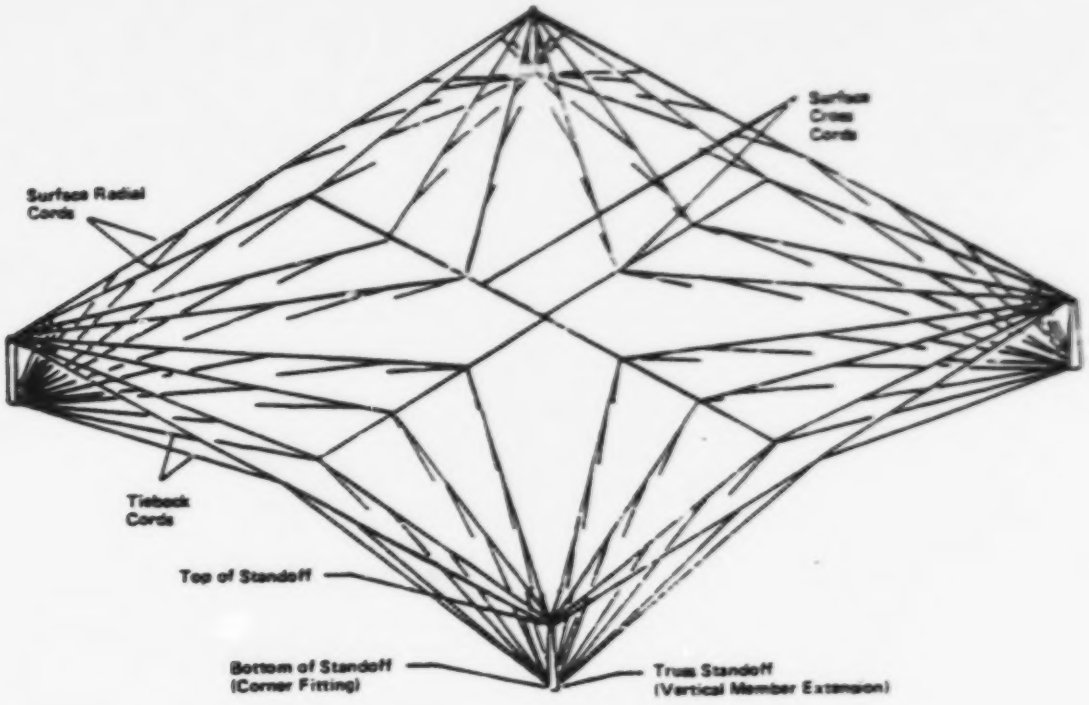

Direct Tieback Tie System

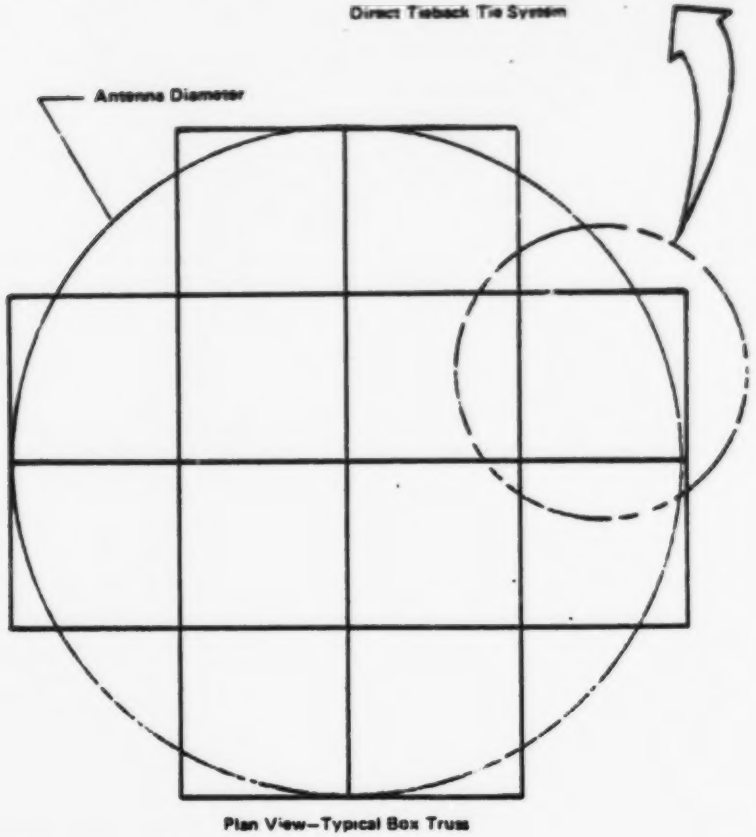

Plan View—Typical Box Truss

Figure 3 Box Truss and Direct Tieback Tie System

1.2 SUMMARY

The result of this task has been a 4.572-m, offset fed box truss reflector with a focal length over diameter (F/D) of 1.5. The achieved surface accuracy using the direct tieback tie system was slightly better than 1/18 of a wavelength at 10 GHz. More importantly, this task advanced box truss reflector technology by providing a physical means for answering many of the concerns associated with incorporating reflective mesh onto a box truss structure. In addition, knowledge into improving the manufacturing technics was realized.

The concerns that were directly examined included:

1) Sewing reflective mesh;

2) Stretching mesh to a desired preload;

3) Assembling and installing the reflector onto the box truss;

4) Setting and verifying the reflector surface;

5) Determining the repeatability of the surface.

Recommendations for improvement resulting from problems during the manufacturing of the reflector includes:

1) Finding a more durable material to replace the graphite cord used to build the tie system;

2) Finding ways to simplify the tieback cord adjustment so that setting the reflector surface is both faster and easier. Specific recommendations are discussed in Chapter 6.0.

2.0 DESIGN AND FABRICATION OF THE REFLECTOR SURFACE

When this task began, the mesh reflector surface was to be installed on the box truss without changing the configuration of the box truss structure. This meant designing and fabricating the reflector surface on equal length standoffs for a center-fed 4.572-m (15 ft) reflector. An F/D value of 2.0 was chosen and the tie cord system would be designed to achieve a surface accuracy compatible with 10 GHz operation and a goal of 1/25 of a wavelength. However, before the installation of the reflector onto the box truss was started, the configuration was changed to meet later test requirements and for comparison to other reflector systems. This modified reflector geometry is a 4.572-m offset-fed reflector with an F/D of 1.5 and offset from the vertex of the paraboloid by 0.61 m (Fig. 4).

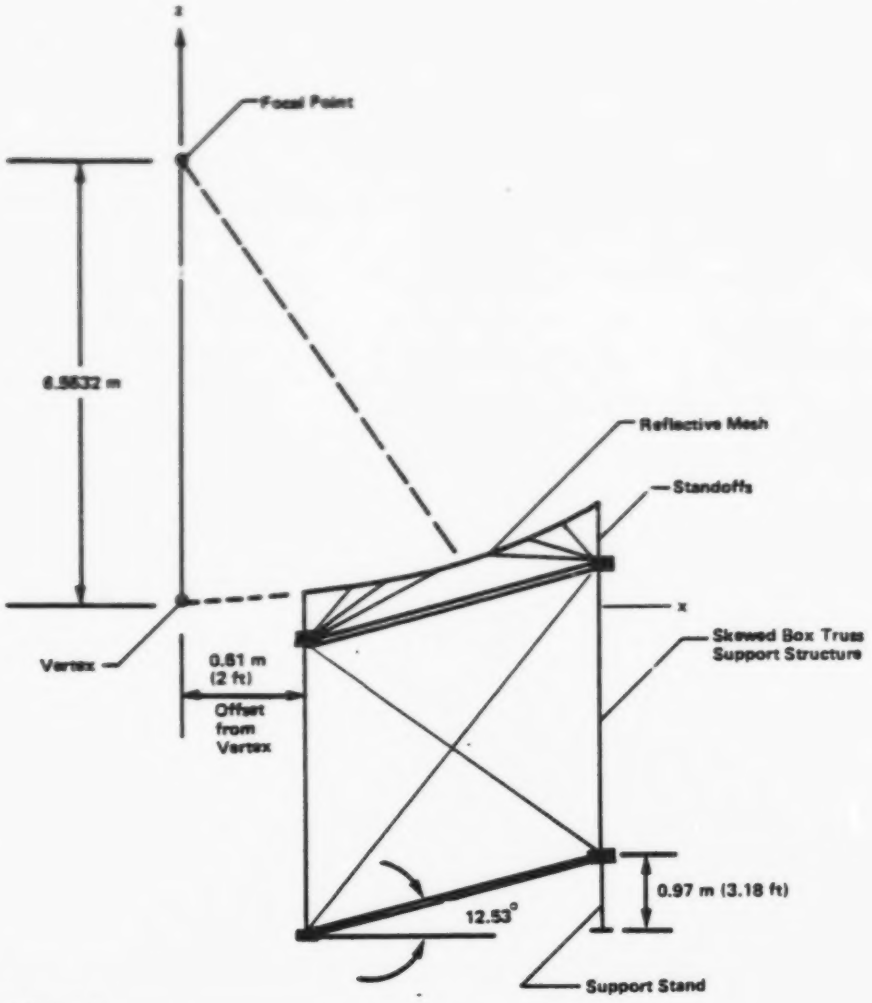

Figure 4
4.572-meter Offset-Fed Reflector Geometry

PRECEDING PAGE BLANK NOT FILMED

Even though the change from center fed to offset fed and the change from an F/D of 2.0 to 1.5 would effect the surface accuracy for a fixed tie spacing, the goal of 1/25 of a wavelength a 10 GHz was still achievable by tightening up the manufacturing tolerance.

2.1 DESIGN OF THE REFLECTOR SURFACE

The first step in designing the reflector was to determine the surface accuracy error budget for the system. The error budget sets the radial tie spacing for the tie system and the required manufacturing tolerance on setting the surface. The values chosen were 55% of the total error are because of pillowing and 45% are because of manufacturing. Generally, a larger value is used for manufacturing, i.e., 75%. However, this would leave only 25% for pillowing, and therefore, increases the number of tie points on the surface. Since cost on this prototype model was an issue, a tradeoff between the cost of fabricating and setting each tie point versus the cost of setting a reduced number of tie points to a closer tolerance was completed. Setting a reduced number of tie points to a closer tolerance was more cost effective.

Using the 55/45 split in pillowing and manufacturing errors resulted in the following:

1) Required surface accuracy = 0.0012-m rms
   at 10 GHz and 1/25 of a wavelength;

2) 55% because of pillowing = 0.00066-m rms,
   45% because of manufacturing = 0.00054-m rms.

Using Equation 1 for determining rms pillowing errors (Ref 1), and solving for TS^2 resulted in a required area bound by the tie points

[1] $\text{rms pillow} = 0.05 * TS^2 / F$

where TS^2 = Mesh Area bound by tie points, m^2
F = Focal length, 6.5532 m
rms pillow = 0.00066 m

of 0.0878 m^2. Note, in the original equation found in Ref 1, TS^2 represented the radial tie spacing squared. However, for the direct tieback tie system, the radial tie spacing along a surface cord does not equal the spacing between radial surface cords, and therefore TS^2 was changed to represent the mesh area bound by a set of four tie points. Once TS^2 was determined, Equation 2 was used to determine a required radial tie spacing of 0.508 m.

[2] $$TS_{rad} = \sqrt{\frac{TS^2}{0.34}}$$

where TS^2 = area bound by tie points, m
TS_{rad} = Radial tie spacing between tie points, m

The constant in Equation 2, 0.34, is based on the relationship between the average area bound by the tie points given a known radial tie spacing.

The manufacturing tolerance is set by three times the required rms manufacturing error or in this case, three times 0.00054-m rms. Therefore, the manufacturing tolerance was set at ± 0.162 cm (0.063 in.).

Table 1 presents a summary of the error budget, tie spacing, and manufacturing tolerance.

Table 1 Error Budget Summary

Required rms Surface Accuracy = 0.121 cm at 10 GHz and 1/25 of wavelength
Pillowing rms Error = 0.066 cm (55%) (0.026 in.)
Manufacturing rms Error = 0.054 cm (45%) (0.021 in.)
Required Radial Tie Spacing = 50.8 cm (20 in.)
Required Manufacturing Tolerance = ± 0.16 cm (± 0.063 in.)

After calculating the radial tie spacing of 0.508 m, the mesh tie system generator (Ref 1), was used to generate the tie point coordinates. The result was a tie system consisting of 212 tie points and 20 catenary points. Later, the number of tie points was reduced to 176 because of a change in catenary depth. This is discussed later in the report. Appendix A shows a complete listing of the point coordinates. The program was run for the center-fed configuration. However, Appendix A shows the coordinates of the offset configuration that were hand generated by taking the center-fed coordinates and translating them into the new configuration. Appendix A shows the constants used for this translation process.

The X and Y coordinates for each point were transferred to the CADDS 4X system and a full-scale plot of the points was produced on vellum. This plot made up the template to be used on the mesh stretching table to locate the tie points, the edge catenaries, and the tops of the standoffs.

The X, Y, and Z coordinates were used to determine the tie cord lengths between tie points and the tieback cord length to each point. Figure 5 and Table 2 summarize the results of the length calculations. As with the mesh template, the surface cords were built to the center-fed configuration and required minor changes to be made during installation. The tieback cord lengths were built oversized, and therefore, could easily be revised to match the new geometry.

Tie System Button Design--After having determined the geometry of the tie system, the next step was to determine a design for attaching the tieback cord to the surface cord. Since the tie cords were to be built of graphite tow, breakage could be expected on some of the cords and therefore the design had to facilitate easy repair.

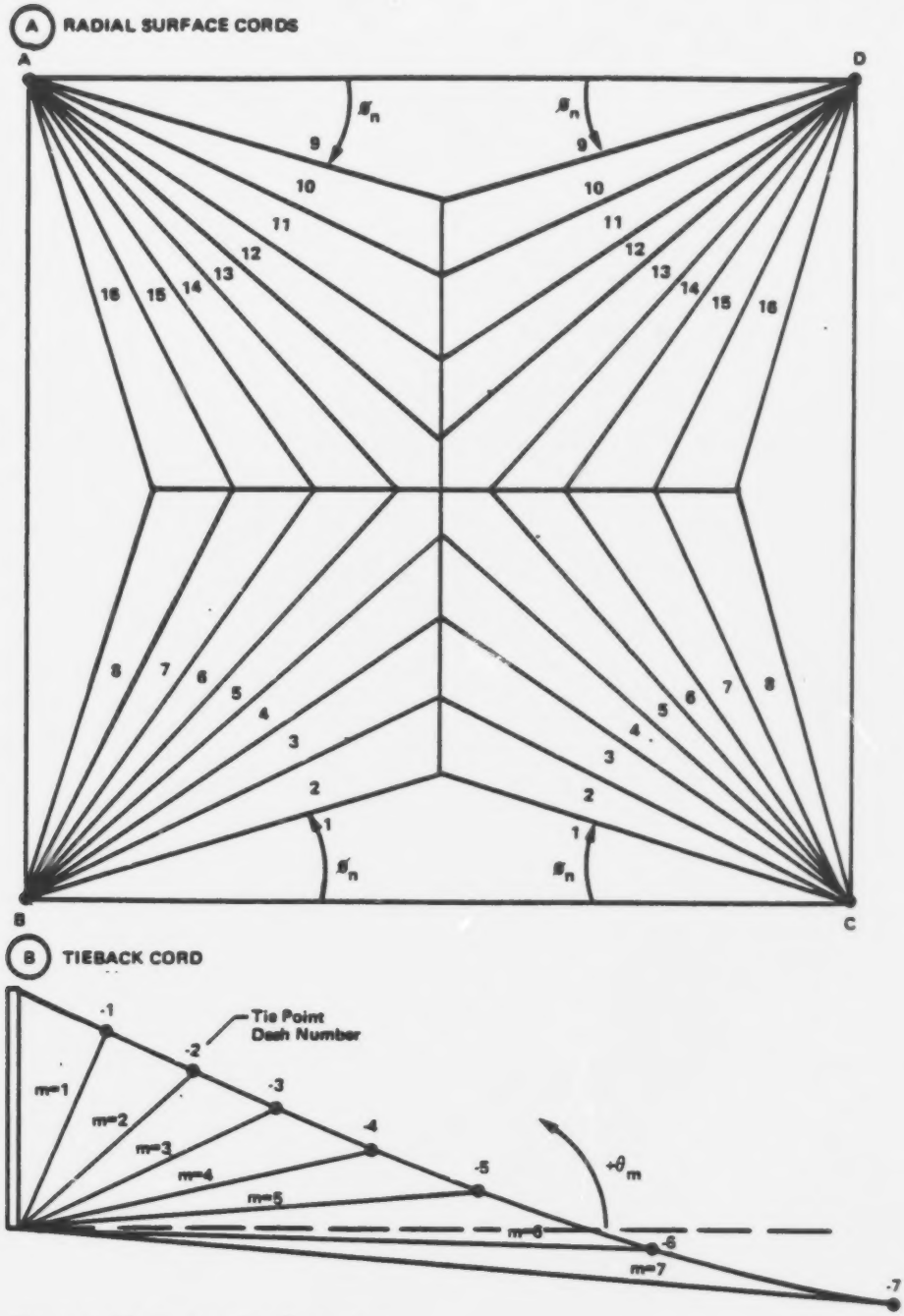

Figure 5 Tie System Configuration

ORIGINAL PAGE IS
OF POOR QUALITY

Table 2 Tie Cord Length

Radial Surface Cords	θ_{ref}, deg	Distance from Top of Standoff, m						
		-1	-2	-3	-4	-5	-6	-7
n= 1	14.4	0.508	1.016	1.524	1.963	2.381	–	–
2	25.4	0.508	1.016	1.524	2.031	2.299	2.566	–
3	34.6	0.508	1.016	1.524	2.031	2.431	2.830	–
4	42.2	0.508	1.016	1.524	2.031	2.538	2.946	3.154
5	48.6	0.508	1.016	1.524	2.031	2.538	2.946	3.154
6	53.2	0.508	1.016	1.524	2.031	2.431	2.830	–
7	62.7	0.508	1.016	1.524	2.031	2.299	2.566	–
8	74.0	0.508	1.016	1.524	1.963	2.381	–	–
9	15.7	0.508	1.016	1.524	1.963	2.381	–	–
10	28.4	0.508	1.016	1.524	2.031	2.299	2.566	–
11	35.6	0.508	1.016	1.524	2.031	2.431	2.830	–
12	43.0	0.508	1.016	1.524	2.031	2.538	2.946	3.154
13	48.4	0.508	1.016	1.524	2.031	2.538	2.946	3.154
14	54.0	0.508	1.016	1.524	2.031	2.431	2.830	–
15	63.2	0.508	1.016	1.524	2.031	2.299	2.566	–
16	74.4	0.508	1.016	1.524	1.963	2.381	–	–

Note: The distance calculations are based on the center-fed configuration.

Tieback Cord	-1		-2		-3		-4		-5		-6		-7	
	L, m	θ, deg	L, m	θ, deg	L, m	θ, deg	L, m	θ, deg	L, m	θ, deg	L, m	θ, deg	L, m	θ, deg
n= 1	0.625	46.2	1.044	24.3	1.514	15.6	1.928	12.0	2.350	9.9	–	–	–	–
2	0.617	46.0	1.039	25.4	1.506	16.8	1.906	12.7	2.258	11.4	2.522	10.5	–	–
3	0.610	46.8	1.031	26.5	1.489	17.9	1.896	13.8	2.360	12.1	2.774	11.0	–	–
4	0.587	47.5	1.024	27.5	1.487	19.0	1.876	14.9	2.494	12.8	2.779	12.1	3.086	11.6
5	0.589	47.9	1.021	27.9	1.488	19.5	1.874	15.4	2.471	13.3	2.778	12.6	3.084	12.1
6	0.615	48.6	1.039	29.0	1.506	20.6	1.901	16.6	2.383	14.8	2.776	13.8	–	–
7	0.636	49.4	1.069	30.3	1.524	22.1	2.012	18.1	2.273	16.9	2.535	16.0	–	–
8	0.666	50.4	1.082	31.8	1.547	23.8	1.961	20.4	2.380	18.4	–	–	–	–
9	0.584	41.1	1.008	18.4	1.483	9.3	1.902	6.5	2.327	3.5	–	–	–	–
10	0.572	39.3	0.986	15.5	1.463	6.2	1.901	1.9	2.226	0.6	2.482	-0.3	–	–
11	0.548	38.1	0.965	13.5	1.446	4.0	1.943	-0.3	2.342	-2.1	2.741	-3.2	–	–
12	0.531	37.2	0.947	12.2	1.427	2.7	1.928	-1.7	2.433	-3.9	2.743	-4.6	3.053	-5.1
13	0.526	36.9	0.948	11.8	1.425	2.2	1.925	-2.2	2.433	-4.4	2.741	-5.1	3.051	-5.6
14	0.536	36.4	0.960	11.0	1.433	1.3	1.933	-3.0	2.334	-4.9	2.733	-5.9	–	–
15	0.546	36.2	0.968	10.6	1.438	0.9	1.941	-3.5	2.207	-4.8	2.474	-5.8	–	–
16	0.556	36.3	0.965	10.8	1.443	1.1	1.864	-2.8	2.291	-4.9	–	–	–	–

Note: Dimension and angles are based on offset configuration—lengths are also based on adjustment fitting geometry.

The solution was to sandwich the surface cord and the end of the tie-back cord between two 1.27-cm diameter 0.508-mm thick aluminum buttons (Fig. 6). The lower button had a 1.27-mm diameter hole drilled in the center so that the tieback cord could be threaded through the center. If a tieback cord should break, which they did too frequently, a new button would be bonded to the bottom. If the surface cord should break, a new surface cord segment, i.e., the piece of cord between two tie points, would be replaced by bonding a new button to the top.

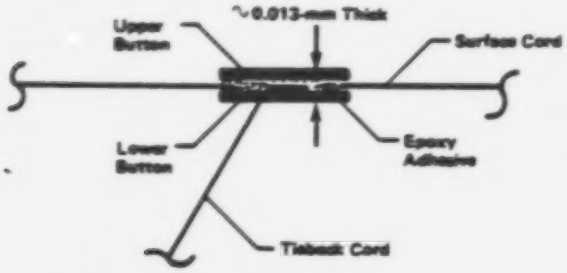

Figure 6 Tie System Button Design

2.2 FABRICATION OF THE REFLECTOR SURFACE

The fabrication of the reflector surface consisted of three basic steps: (1) stretch and mark the mesh; (2) install the edge catenaries; and (3) build the tie system.

2.2.1 Mesh Surface Fabrication

The mesh material is a tricot-knit, 0.003-cm diameter, gold-plated molybdenum monofilament wire mesh that has 5.5 openings/cm. The mesh has the desirable properties of high rf reflectivity, corrosion resistance, low weight, wrinkle resistance, low-spring rate, puncture resistance, and radiation resistance. Figure 7 shows the mesh knit. An 2.286 by 4.572-m wooden table was fabricated and used for stretching the mesh surface, installing the edge catenaries, and marking the tie point locations on the mesh. The vellum template locating the tie points, edge catenaries, and top of standoffs was placed over the table. The table was then covered with Mylar and all edges were smoothed with Mylar tape to minimize the friction between the mesh and the table.

ORIGINAL PAGE IS
OF POOR QUALITY

Figure 7 Tricot Knit Weave

Since one of the features to be demonstrated in this task was sewing seams in reflective mesh, a 0.61 by 1.219-m patch was sewn into one corner (Fig. 8). It was sewn to the main body of the mesh by first stretching the patch to the appropriate tension level, then applying 5.08-cm wide Mylar tape to the raw edges to be sewn. The same was done to the main body of the mesh surface. The taped edges were then pressed together with the mesh edges sandwiched in between. A hand held sewing machine using nylon sewing thread was then used to produce the final seam (Fig. 9). The tape edge was used as a guide to assure a straight seam. After the sewing was complete, the tape was removed and the excess mesh material was trimmed to approximately 0.6-cm. Because both pieces of mesh had been prestretched before being sewn, the seam did not need to stretch. The final result was an almost invisible seam that produced no apparent discontinuities in the surface.

Once the sewing process was complete, the entire mesh was laid on the stretching table with the material bias at 45 deg to the sides of the table (Fig. 8). The mesh was oversized, approximately 5.5 by 5.5 m, so that the mesh edges would overhang the table to allow for attachments of weights for stretching the mesh. A total of 540 weights, each being 45.5 grams, were hung 5.08 cm apart along the mesh periphery to produce a biaxial tension field in the mesh of approximately 0.088 N/cm. This higher biaxial tension field was used to compensate for gravity. However, the level was too high and caused the mesh to stretch to the point were it was no longer pliable. Therefore, each weight was reduced to 24 grams resulting in a biaxial tension field of approximately 0.046 N/cm. The table was then subjected to a vibration cycle. The

vibration was induced by two Vibrolator air-driven motors powered by 6.895×10^5 N/m^2 nitrogen pressure. The vibration, coupled with the weights, caused the mesh to fully expand and remain under tension.

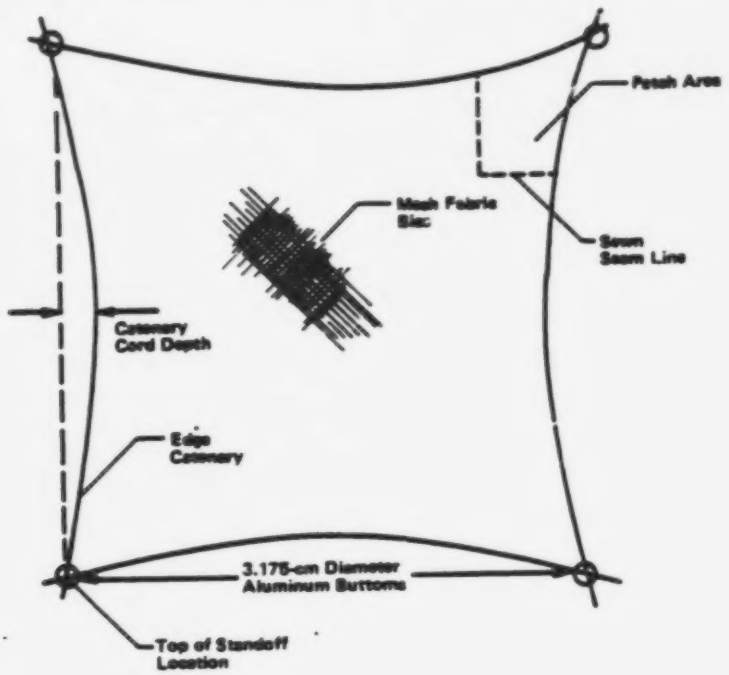

Figure 8 Mesh Fabric

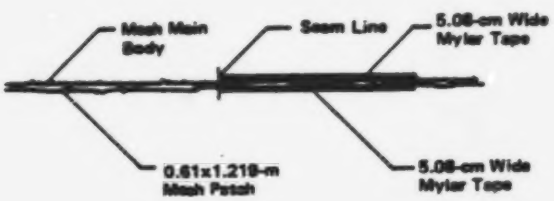

Figure 9 Reflective Mesh Seam

Next, catenary cords (12000 tow teflon-coated Celion graphite cord) were laid on the mesh per the template and whipstitched in place with standard black sewing thread using about a 2.5-cm loop. This was accomplished on half of the mesh at a time. The catenaries were then preloaded with approximately 13.6 kg, i.e., the force needed to react the biaxial tensioned mesh.

Once the catenary cords were in place and preloaded, a 3.175-cm diameter, 0.508-mm thick aluminum button was bonded to the mesh and each end of the catenary cord. The Teflon coating on the graphite cords was etched for bonding using Tetra-etch (Gore) and the bonding adhesive

was Hysol EA934NA. The location of the buttons corresponded to the tops of the standoffs (Fig. 8). After bonding, a clearance hole was drilled in each button for mechanical attachment of the mesh surface to the top of the standoffs.

The final step was to mark the mesh for each tie point location by tying a black thread to the mesh at each location dictated by the template. The thread markings served as locators for pulling each tieback cord through the mesh during installation of the tie system onto the mesh surface.

2.2.2 Tie System Fabrication

The tie system was built using 3000 tow Celion Teflon-coated graphite cord and 0.508-mm thick by 1.27-mm diameter aluminum buttons. Using the lengths in Table 2, lines were drawn on the template, which connected the tie points along each surface cord and denoted the various angles required by the system (Fig. 10).

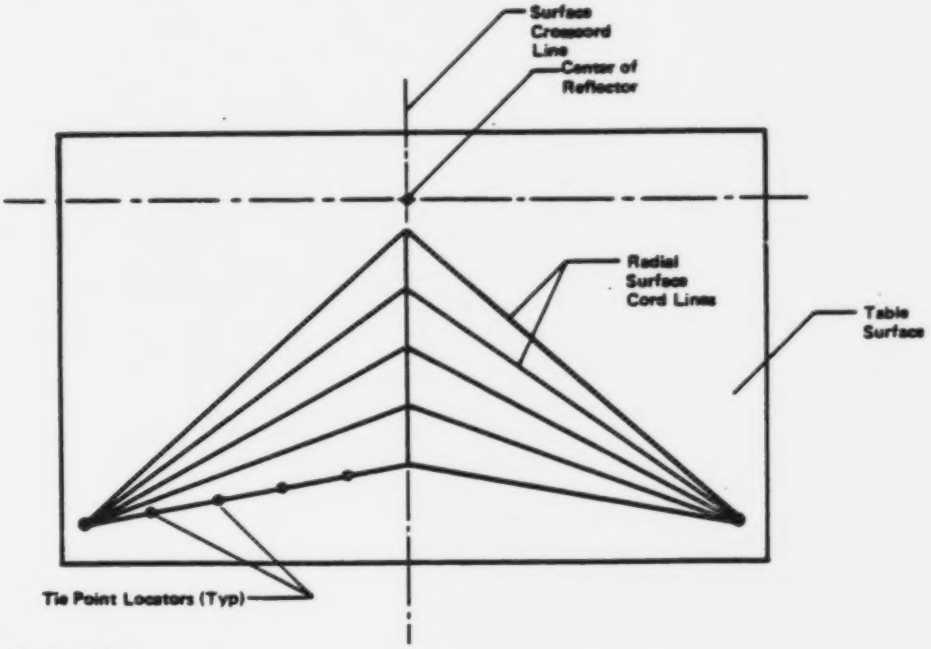

Figure 10
Tie System Fabrication Table (½ of Tie System "Fishbone")

The first operation involved cutting each tieback cord and surface cord to the proper length. Surface cord lengths were obtained from the template. Tieback lengths are found in Table 2. However, the tieback cords were cut 30-cm oversize.

The next step involved attaching each tieback cord to its corresponding radial surface cord. This was accomplished by first taping the radial surface cord onto the template. Then, at each tie point, a single tieback cord was threaded through an aluminum button with a hole. The

tieback and radial surface cord were then sandwiched between a top and bottom button. They were bonded with Hysol EA934NA epoxy adhesive and cured for 16 hours minimum at room temperature using a deadweight system. The tieback cords were bonded at the appropriate angle to the surface cords, shown in Table 2, to assure that when pulled they would not have to bend at the attachment point.

After all the tieback cords had been bonded to the 40 radial surface cords, the surface cross cords were laid on the template and the two radial surface cords and two tieback cords were bonded at the appropriate locations. The radial surface cords were bonded to the surface cross cords at the appropriate angle to minimize any bending of the cord at the attachment point.

Before bonding, the bond area of all the buttons was grit blasted and primed with BR127 epoxy primer. The primer was cured at 250°F ± 10°F for 30 to 60 minutes. The Teflon coating on the graphite cords was etched with Tetra-etch for bonding at each of the tie point locations.

The end result was a pair of "fishbone" surface cord assemblies, the X set and Y set with respect to the reflector coordinate system. When the adhesive was cured, each "fishbone" was individually rolled on separate 7.6-cm diameter spools for simplified handling and transportation.

2.2.3 Box Truss Standoffs and Tie Cord Adjustments

Before the reflector could be installed on the box truss, the standoffs and tieback cord adjustment mechanisms needed to be designed and built. The height of each standoff was chosen to be 0.5715 m (22.5 in.). This value was calculated as the optimum standoff height by the Mesh Tie System Generator (Ref 1). Included in the 0.5715-m standoff length was an adjustment fitting to allow adjustment of each tieback cord.

Tieback Cord Adjustment Hardware--The tieback cord adjustment hardware consisted of two components: pairs of 0.3175-cm (1/8-in.) diameter coarse adjustment tubes and 2-56 fine adjustment set screws, one pair per tieback cord (Fig. 11), and an adjustment fitting made up of aluminum angle, one per standoff (Fig. 12).

The coarse adjustment tubes are 5.715-cm long 304 stainless tubing. The OD of the tube was threaded with a 6-32 die to establish a grip area for the O-ring stop (Fig. 11). The coarse adjustment tube adapted to the adjustment fitting (Fig. 13). The clearance holes drilled in the aluminum angle allowed the tubes to move their full length in the adjustment fitting. Since the tieback cords were under low tension when the mesh was in a properly configured paraboloid, O-ring stops were suffi- cient to prevent the coarse adjustment tubes from pulling out of the adjustment fitting. The O-ring size was 2-004 (type Buna 71).

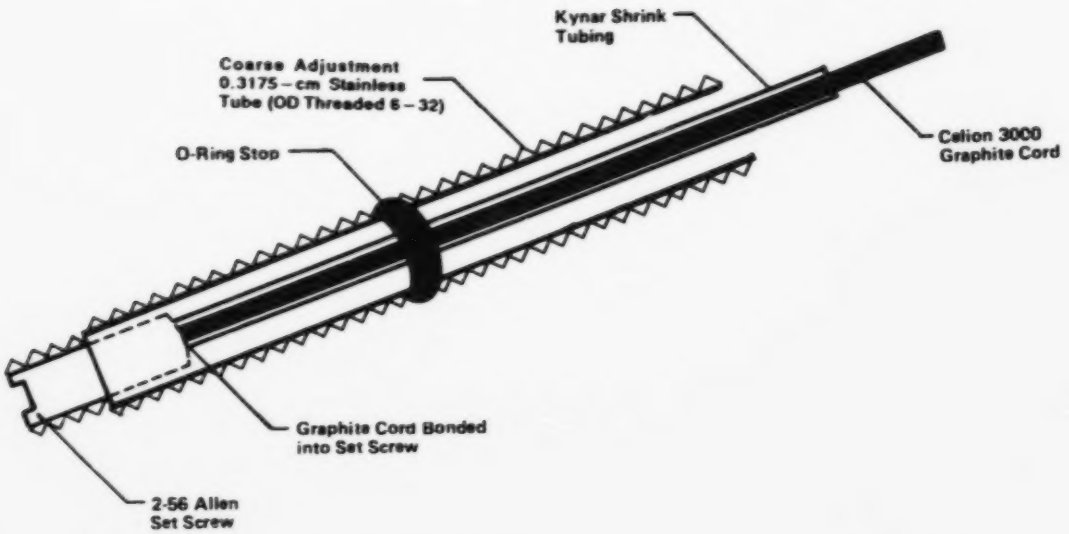
Kynar Shrink Tubing
Coarse Adjustment 0.3175-cm Stainless Tube (OD Threaded 6-32)
O-Ring Stop
Celion 3000 Graphite Cord
Graphite Cord Bonded into Set Screw
2-56 Allen Set Screw

Figure 11 Tieback Cord Adjustment Hardware

The fine adjustment, 2-56 allen set screws, are 0.64-cm long and screw inside the outer end of the coarse adjustment tube. The inside end of the allen screw contained a 0.102-cm diameter hole into which the graphite tieback cord was bonded, using Shell EPON 828 resin with 10% of diethylene triamine (DETA) catalyst. The graphite cord was etched with Tetra-etch to remove the Teflon coating before bonding. The fine adjustment yields $\pm$ 1.78-mm of movement at the mesh tie points.

The area of the graphite cords, which was located inside of the coarse adjustment tubes, was protected from fraying by heat shrinkable tubing (Kynar 0.119-cm diameter).

The adjustment fitting was fabricated from 0.635-cm (1/4-in.) thick aluminum angle and had 8.15-cm legs. Each side of the angle had 27 holes, each drilled at a compound angle. The holes were drilled at compound angles to accept the coarse adjustment tubes. The drilling was accomplished using a milling machine with a two-axis tilt head. Each hole location was marked on the outside faces of the angle with a height gage. The angle was then placed in the mill. Each hole was started with a 0.635-cm (1/4-in.) starter drill and drilled to 0.3175-cm (0.125-in.) with a 0.3175-cm (1/8-in.) bit and reamer. This allowed a slide fit for the coarse adjustment tube.

Box Truss Standoffs--The overall standoff assembly is presented in Figure 14. The assembly was constructed from aluminum plate, 3.81-cm (1.5-in.) aluminum tubing, and 0.635-cm (1/4-in.) mild steel plate.

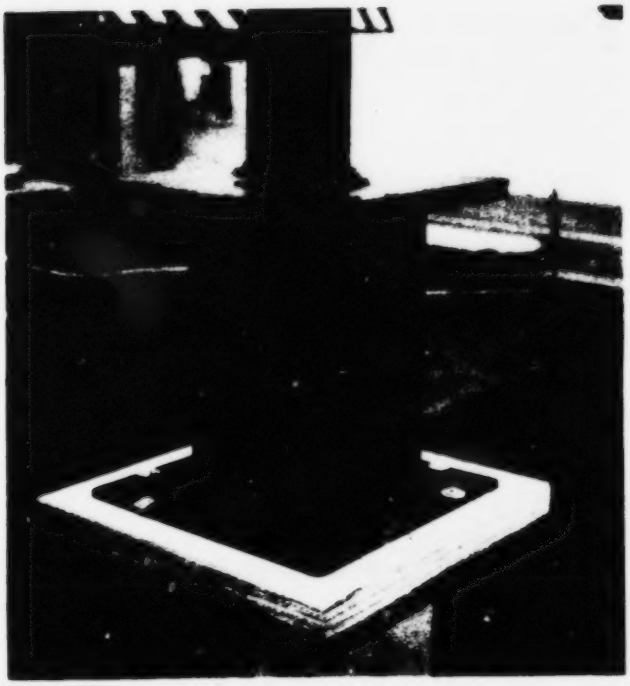

Outside View

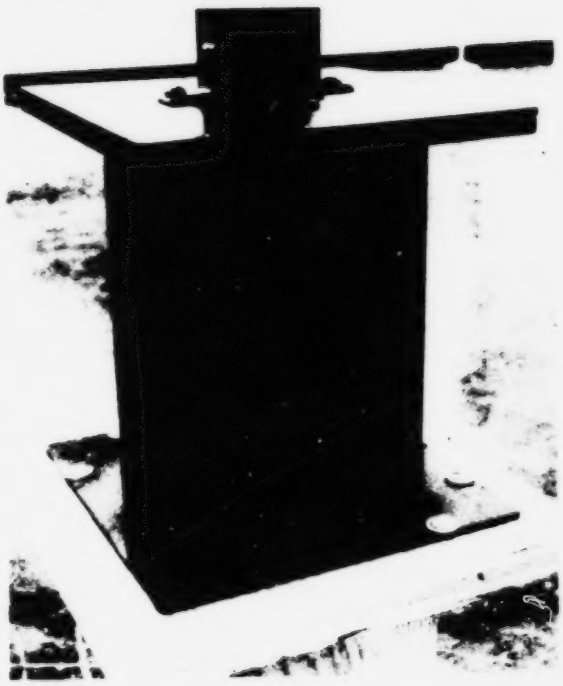

Inside View

Figure 12 Aluminum Adjustment Fitting

ORIGINAL PAGE IS
OE POOR QUALITY

ORIGINAL PAGE IS
OF POOR QUALITY

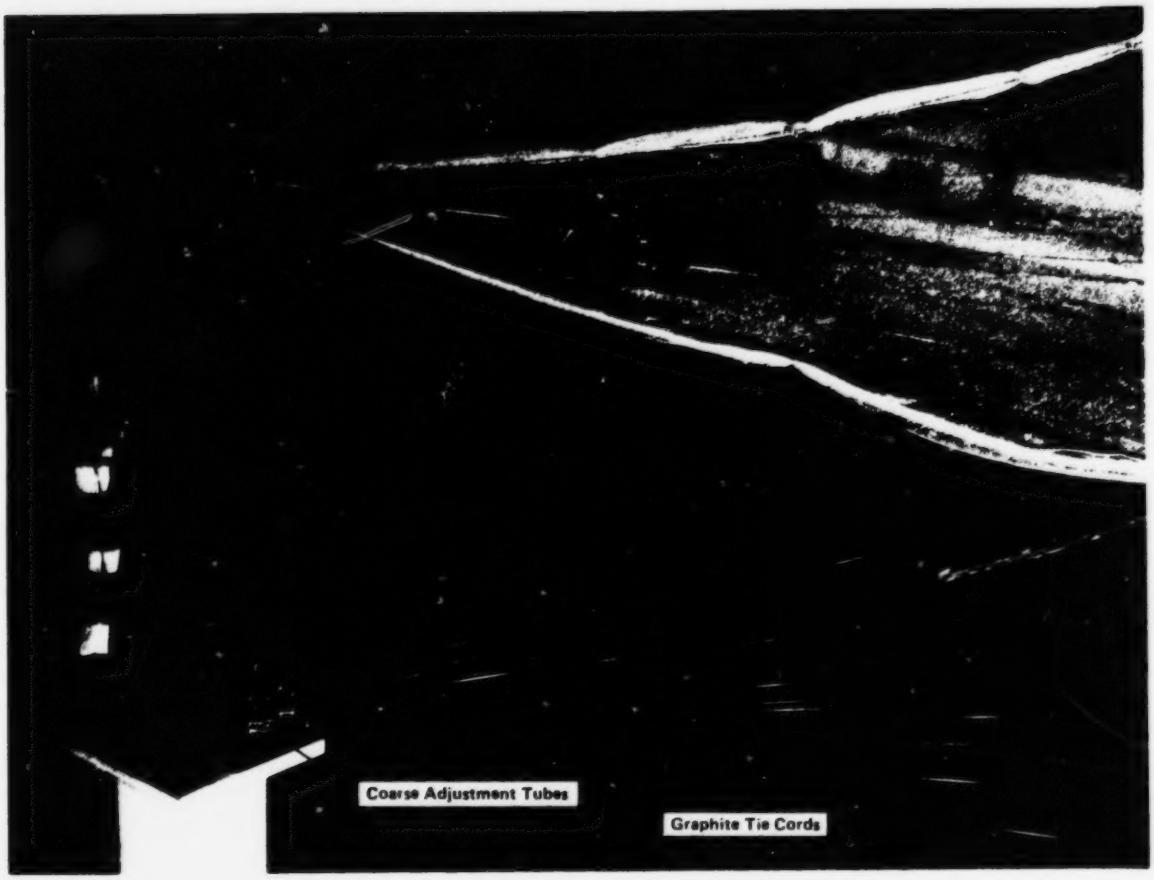

Figure 13 Attachment Fitting with Adjustment Hardware Installed

The mesh attachment plates were tilted 22 deg toward the reflector center on the upper standoffs and the lower standoffs were tilted 10 deg towards each other. This closely approximated the curvature of the paraboloid at the top of the standoffs and allowed the mesh surface to assume the paraboloidal shape without having to bend over a shape edge. The 3.175-cm aluminum discs were mechanically attached to the mesh attachment plates with 6-32 screws. The notches at the radius of the mesh attachment plates were guides for the surface cords and their weights. All plates were attached to the 3.81-cm (1.5-in.) square tubes with aluminum angles and screws.

The 0.3175-cm (1/8-in.) flat plates provided both load transfer into the graphite truss and bending stability. The 0.635-cm (1/4-in.) steel plate was needed for more rigidity since the 3.81-cm (1.5-in.) tube did not extend through the adjustment hardware box (Fig. 12). This was done to allow greater access to the adjustment screws. Figure 12 also shows a stability leg opposite of the adjustment fitting.

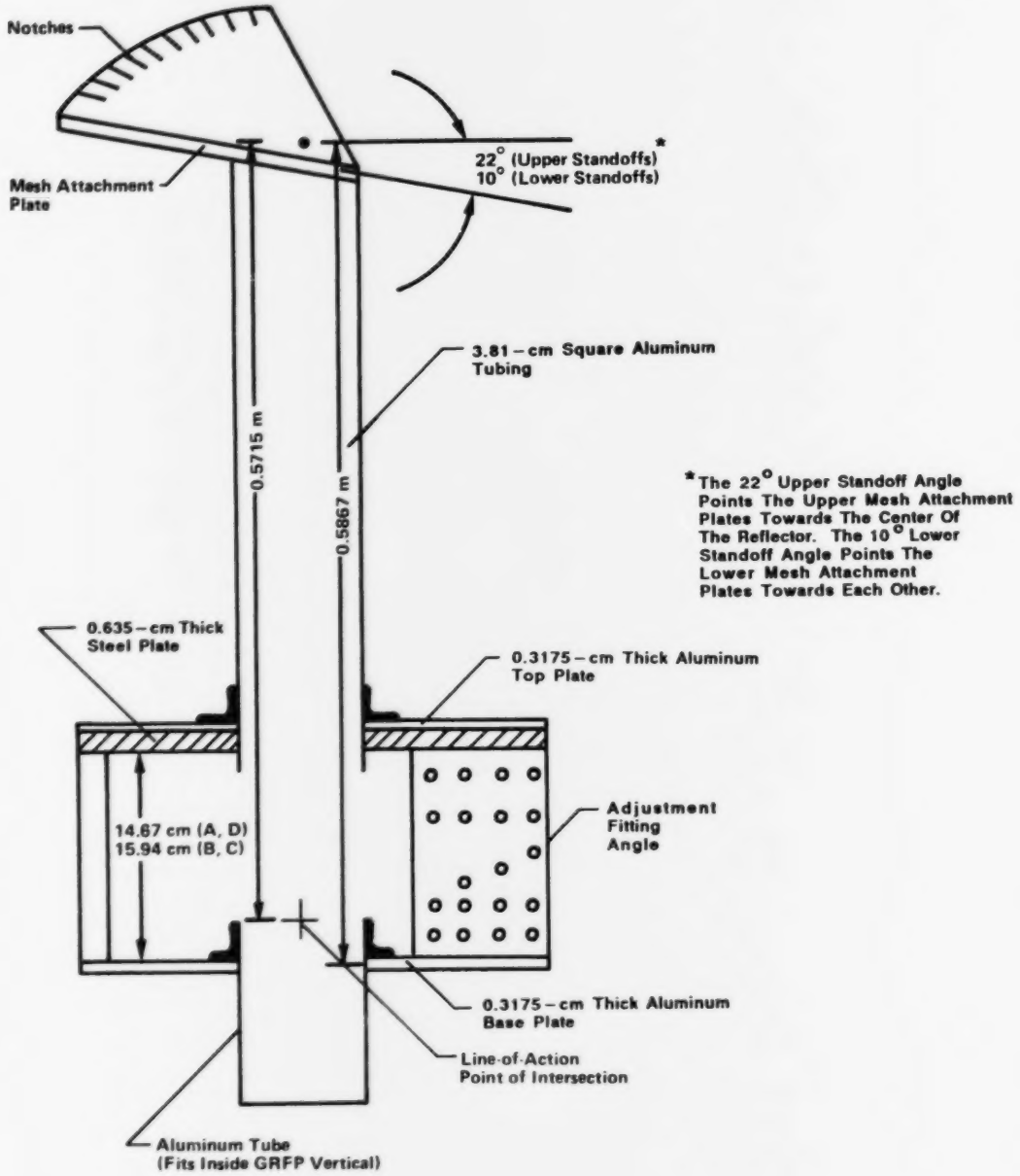
Notches
Mesh Attachment Plate
22° (Upper Standoffs)*
10° (Lower Standoffs)
3.81-cm Square Aluminum Tubing
0.5715 m
0.5867 m
*The 22° Upper Standoff Angle Points The Upper Mesh Attachment Plates Towards The Center Of The Reflector. The 10° Lower Standoff Angle Points The Lower Mesh Attachment Plates Towards Each Other.
0.635-cm Thick Steel Plate
0.3175-cm Thick Aluminum Top Plate
14.67 cm (A, D)
15.94 cm (B, C)
Adjustment Fitting Angle
0.3175-cm Thick Aluminum Base Plate
Line-of-Action Point of Intersection
Aluminum Tube (Fits Inside GRFP Vertical)

Figure 14 Standoff Assembly

The most critical dimension of the standoff assembly was the 0.5715-meter from the attachment point of the mesh to the point of intersection of the tieback cords (Fig. 14). This lines-of-action intersection point was 1.524-cm above the base plate to gain more clearance for the coarse adjustment tubes. The adjustment fitting aluminum angle varied from 14.67-cm high for the upper standoff assemblies to 15.94-cm for the lower standoffs. The aluminum tube below the base plate was machined to 3.49-cm to allow for a slip fit into the top end of the square tube vertical member of the graphite truss.

ORIGINAL PAGE IS
OF POOR QUALITY

3.0 INTEGRATION OF REFLECTOR AND SURFACE SETTING

Integration of the reflector onto the box truss and setting the surface was completed in two main steps. First, the mesh and tie system were assembled onto the standoffs and the surface initially set with the standoffs installed in ground level wooden stands. Then the standoffs were installed in the box truss and a final surface setting was completed. This two-step process was used so no major scaffolding was needed to mate the tie system to the mesh or to set the surface.

3.1 WOODEN STANDS FOR MESH ASSEMBLY

Wooden positioning stands were fabricated to support the standoffs during the mating process of the tie system to the mesh fabric. They consisted of a 2.54-cm (1-in.) plywood base with four leveling screws, a tower made from 2x4 lumber and supported with pine gussets, and a 1x6 pine top plate with a centered square hole to which the standoffs were bolted for support.

A pair of support boxes were fabricated to elevate the upper standoffs 0.97-m higher than the lower standoffs. They were constructed from 2.54-cm (1-in.) plywood with access holes for weights and manipulation of the four leveling screws (Fig. 15).

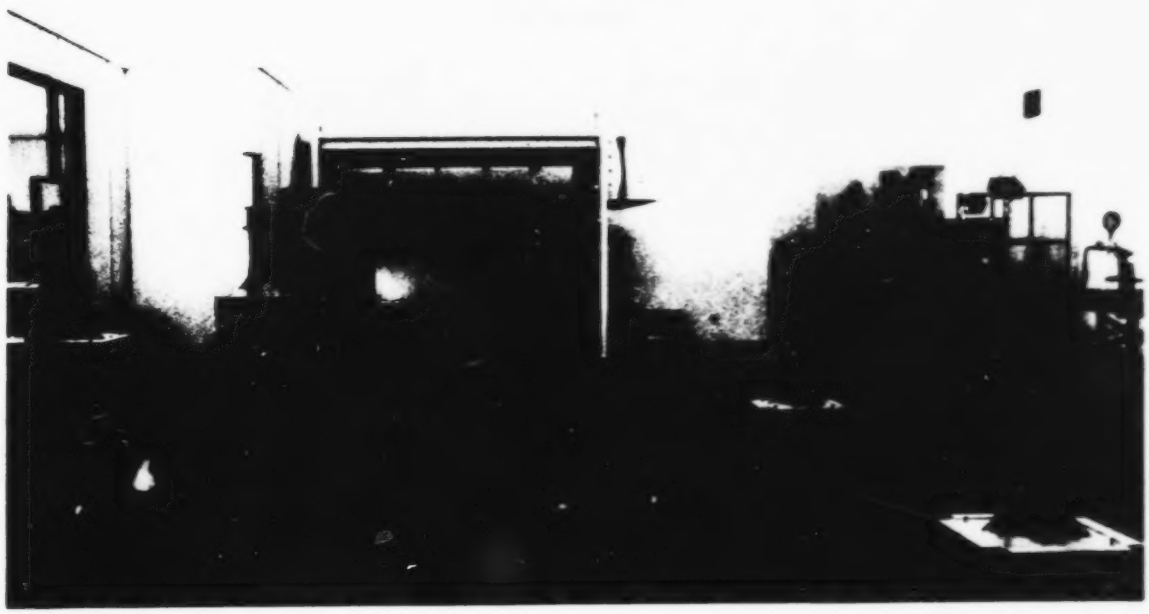

Figure 15 Wood Stands and Standoffs

The wood stands were positioned with the aid of a surveyor's transit. The stands were first leveled and then raised or lowered to bring the two lower stand top plates into the same plane. The upper stands were then adjusted to the same plane and 0.97- m higher than the lower top plate plane. This configured the standoffs for a 12.53-deg skew of the box truss (Fig. 4).

The standoffs were then adjusted to meet dimensional requirements. A standard tape measure was used for locating distances. The standoffs were set for 4.572-m between the upper set of two. Adjustments were made for obtaining a distance of 4.569-m between lower and upper standoffs on the 12.54 deg angle and 4.466-m between lower and upper standoffs in the horizontal plane. Diagonally, the setup measured 6.464-m from upper standoff to lower standoff.

3.2 INSTALLING THE MESH AND TIE SYSTEM ONTO THE STANDOFFS

The mesh fabric was installed on the corner fittings by mechanically attaching the 3.175-cm aluminum discs to the standoff top plates with a 6-32 screw. Next, the mesh was released from the two lower standoffs and carefully folded back so that one of the tie system's "fishbone" assemblies could be installed starting at the upper side and working down. The tieback cords were threaded through the mesh fabric at the premarked locations denoted by the black thread. As the tie system was installed the mesh was pulled back into place until finally all tieback cords were through the mesh and the mesh was reattached to the standoffs. The same approach was used to install the second "fishbone" assembly only this time the mesh was released from one upper and one lower standoff. Figure 16 shows the reflector surface installed on the standoff before installing the tieback cords into the adjustment fitting.

When the installation was complete, the tieback cords were then cut to the required lengths (Table 2), the ends prepared for bonding with Tetra-etch and the adjustment hardware was bonded to the tie cord ends as previously described in Subsection 2.2.3. The tieback cords were mated with the standoff adjustment fitting by inserting the coarse adjustment tube [illegible] the appropriate hole in the angle. A 113.4-gram weight was susp[illegible] from each of the surface cords to assure the preload in each cord was equal to the tension of the mesh.

At this point, two problems occurred. First, the 10.16-cm deep catenaries that were originally installed for the center-fed configuration could not be pulled down into shape for the offset reflector without creating extremely high tension levels in the catenaries . Second, the tieback cords going to the upper standoffs were slack and the tieback cords going to the lower standoffs were extremely tight, i.e., it appeared the entire tie cord system was positioned too far toward the upper standoffs.

ORIGINAL PAGE IS
OE POOR QUALITY

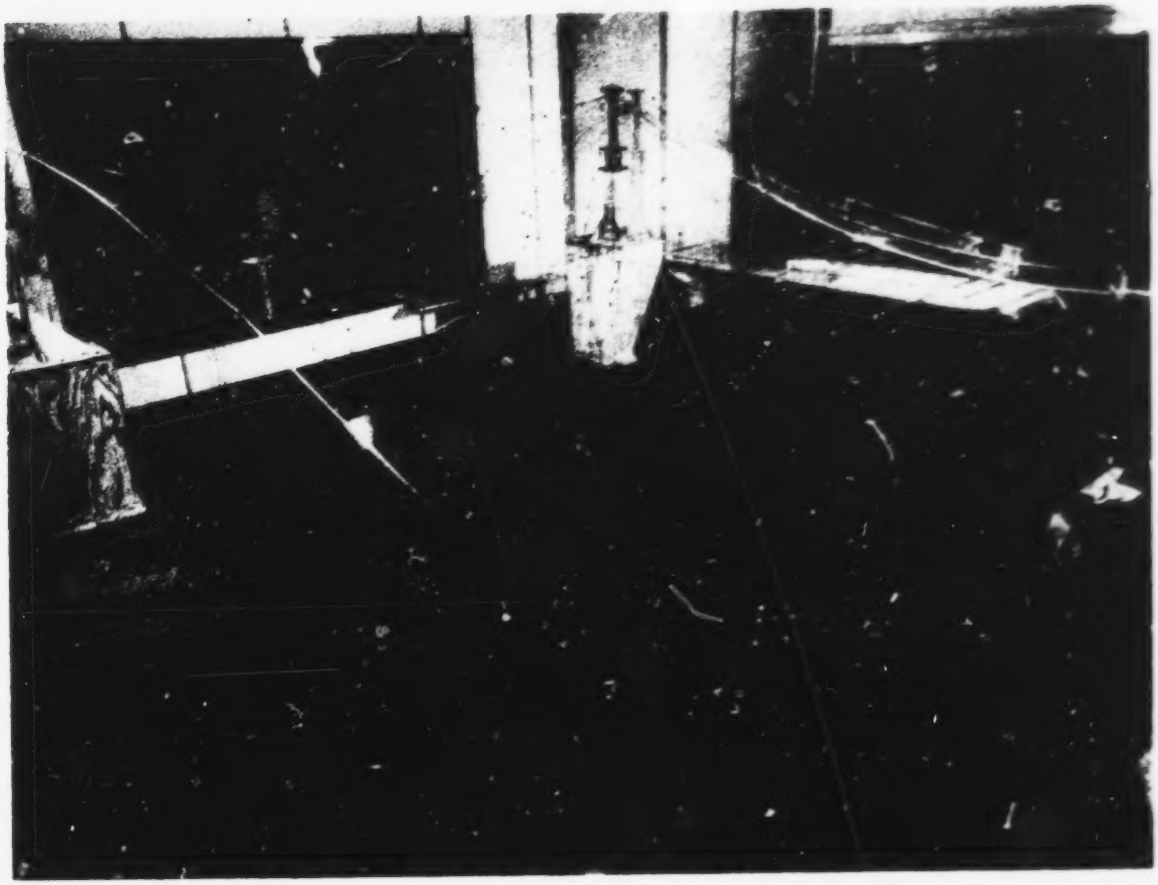

Figure 16 Reflector Surface before Tie System Tensioning

To fix the catenaries, new catenary cords were sewn into place at a nominal 30.5-cm depth using a tighter whipstitch loop to provide more uniform mesh tension. Since catenary tension is inversely proportional to the depth, changing the edge catenary depth from 10.16 to 30.5 cm lowered the catenary pretension level to a manageable level. The new catenary depth of 30.5 cm was chosen using engineering judgment. Also, since the actual distance between tops of standoffs, i.e., the distance along the paraboloid, had increased going from the center-fed to offset fed configuration, the mesh tension had increased and therefore needed to be reduced. This was accomplished by drilling new attachment holes in the standoff top plates. The 3.175-cm aluminum discs were each moved 1.0-cm toward mesh center.

This change had several effects:

1) The catenary depth changed from 31.24 to 33.53 cm;

2) The diagonal mesh dimension changed from 6.454 to 6.450 m;

3) The gravitational droop at mesh center changed from 8.9 to 15.24 cm.

To verify that the change had reduced the mesh tension to the proper level, the approximate droop in the center of the reflector was hand calculated. The result showed that at 0.0464 N/cm, the mesh should sag 14.48 cm, close to the 15.24 cm measured.

To fix the tie system, it was necessary to relocate all the tie points on the mesh surface. Again, the problem occurred because of the change in configuration. For the upper half of the reflector, which is further up on the paraboloid in the offset configuration, the distance between any single tie point and the bottom of the standoff had decreased. The opposite was true for the lower half of the reflector. Therefore, new tie point locations were approximated and the mesh was marked to identify each new position. The location changes are presented in Table 3. Overall, the tie system was moved approximately 6.4 cm toward the lower standoffs. When the tie system was inplace, the tieback cords were again inserted into the adjustment fitting. The lengths appeared to be acceptable. However, when the tieback cords were drawn into tension and the mesh surface began to assume a parabolic shape, some of the surface cords remained slack. The solution to this problem required a third and final tie system relocation.

Table 3 Tie Point Location Change

Tie Point	Delta, cm	Tie Point	Delta, cm	Tie Point	Delta, cm	Tie Point	Delta, cm
B&C 1-1	1.346	B&C 1-2	2.697	A&D 9-1	1.346	A&D 9-2	2.697
B&C 1-3	4.054	B&C 1-4	5.202	A&D 9-3	4.054	A&D 9-4	5.202
B&C 1-5	6.350	B&C 2-1	1.247	A&D 10-5	6.350	A&D 10-1	1.247
B&C 2-2	2.502	B&C 2-3	3.759	A&D 10-2	2.502	A&D 10-3	3.759
B&C 2-4	5.019	B&C 2-5	5.685	A&D 10-4	5.019	A&D 10-5	5.685
B&C 2-6	6.350	B&C 3-1	1.130	A&D 10-6	6.350	A&D 11-1	1.130
B&C 3-2	2.266	B&C 3-3	3.404	A&D 11-2	2.266	A&D 11-3	3.404
B&C 3-4	4.547	B&C 3-5	5.448	A&D 11-4	4.547	A&D 11-5	5.448
B&C 3-6	6.350	B&C 4-1	1.011	A&D 11-6	6.350	A&D 12-1	1.011
B&C 4-2	2.032	B&C 4-3	3.053	A&D 12-2	2.032	A&D 12-3	3.053
B&C 4-4	4.077	B&C 4-5	5.103	A&D 12-4	4.077	A&D 12-5	5.103
B&C 4-6	5.725	B&C 4-7	6.350	A&D 12-6	5.725	A&D 12-7	6.350
B&C 5-1	0.955	B&C 5-2	1.915	A&D 13-1	0.955	A&D 13-2	1.915
B&C 5-3	2.875	B&C 5-4	3.840	A&D 13-3	2.875	A&D 13-4	3.840
B&C 5-5	4.808	B&C 5-6	5.624	A&D 13-5	4.808	A&D 13-6	5.624
B&C 5-7	5.984	B&C 6-1	0.813	A&D 13-7	5.984	A&D 14-1	0.813
B&C 6-2	1.631	B&C 6-3	2.457	A&D 14-2	1.631	A&D 14-3	2.451
B&C 6-4	3.274	B&C 6-5	3.924	A&D 14-4	3.274	A&D 14-5	3.924
B&C 6-6	4.572	B&C 7-1	0.622	A&D 14-6	4.572	A&D 15-1	0.622
B&C 7-2	1.247	B&C 7-3	1.872	A&D 15-2	1.247	A&D 15-3	1.872
B&C 7-4	2.499	B&C 7-5	2.832	A&D 15-4	2.499	A&D 15-5	2.832
B&C 7-6	3.162	B&C 8-1	0.373	A&D 15-6	3.162	A&D 16-1	0.373
B&C 8-2	0.747	B&C 8-3	1.120	A&D 16-2	0.747	A&D 16-3	1.120
B&C 8-4	1.120	B&C 8-5	1.755	A&D 16-4	1.120	A&D 16-5	1.755

ORIGINAL PAGE IS
OF POOR QUALITY

The approach used required that the tie system be isolated from the mesh fabric. First, the tieback cords were released from the adjustment fitting. Then, each surface cord had a 113.4-gram weight suspended from its termination end at the standoff. This placed the entire surface cord system into tension and resulted in the surface cords moving upward, suspended above the mesh surface. This positioned all the surface cords in one flat plane, above and isolated from, the mesh surface. The fabric was also in a static state under tension and free from any surface cord influence.

At this point, the surface cross cords were aligned to the center of the mesh surface in the offset direction and aligned in the other direction to be perpendicular. The system was now prepared to relocate the tieback cord positions. The tieback cords were extracted from the mesh individually and reinserted through the mesh at a point directly below the tie point and in plane with the mesh surface.

After all the tieback cords were through the mesh, they were inserted into the adjustment fitting and held in place with the O-ring stops. This caused the mesh to be drawn into a roughly paraboloidal shape and placed the surface cords into proper tension. Figure 17 shows the final reflector integrated on the standoffs. The next step was to set the surface.

Figure 17 Reflector Surface with Tie System Installed and Tensioned

3.3 AIMS THEODOLITE MEASURING SYSTEM

Before actual adjustment of the mesh surface, an initialization of the theodolite system was compulsory. The theodolite system was a K&E (Keuffel & Esser) AIMS-R/T (real-time measuring system). It was comprised of two encoder-type optical theodolites with portable base stands. The theodolites were linked to a computer/video monitor that contained the capability of performing parabolic functions.

The theodolite system initialization involved:

1) Theodolite coarse and electronic leveling;

2) Pointing both theodolites at a common azimuth reference;

3) Pointing the theodolites at each other to give the computer the location of each theodolite;

4) Entering into the computer a scale factor of 68.00 in. by pointing the theodolites at the 1-in. and 69-in. marks on a calibrated scale;

5) Pointing the theodolites at reference targets on each lower standoff of the mesh assembly;

6) Entering into the computer the X, Y, and Z coordinates (in in.) of the zero point of the parabola;

7) Entering into the computer the coordinate dimensions of five points of the parabola (in in.), which are minus X, plus X, zero, plus Y, and minus Y;

8) Setting up the computer stack sequence by pointing the theodolites at five imaginary points that simulate the previously entered coordinate dimensions;

9) Using a function key that allows the computer to calculate the theoretical parabola from the input and theodolite data.

The theodolite system required reinitializing approximately every 2 days because of error accumulation from handling and floor movement.

3.4 COARSE ADJUSTMENT OF MESH SURFACE

After theodolite initialization, coarse adjustment of the mesh surface was begun. The technique proceeded by pointing the theodolites at each target, i.e., a tie point button twice. First in the direct mode and next in the reverse mode. The two measurements are automatically averaged by the computer to reduce the pointing error by half. To assure that each theodolite operator was pointing at the same target, each tie point was identified with a label generated from Figure 5.

Except for the tie points along the surface cross cords, the labeling was based on the standoff letter, the radial surface cord number, and a dash number. For example, target C5-1 is the first tie point out from the "C" standoff along the number 5 radial surface cord. C5-6 would be the sixth tie point out from the same standoff along the same radial surface cord. For the tie points along the surface cross cord, the label was based on the standoff letters and a dash number, i.e., AD-1 is the first tie point on the surface cross cord between standoffs "A" and "D." The parabolic function was calculated and the results were displayed on the monitor. The display included the pointing error of the theodolites (X.XXXX in.) and the deviation from the required paraboloid, either plus or minus (X.XXXX in.).

The tie point being measured was then adjusted up or down (plus or minus) to within 0.254 cm of the paraboloid. This was achieved by moving the coarse adjustment tube (Fig. 11) either in or out of the standoff adjustment hardware angle. The O-ring stop was repositioned accordingly to prevent the adjustment tube from being pulled free from the angle while under tension.

The tie points were adjusted in a circular pattern beginning at the center of the reflector. The center four points were adjusted first (AB-4, BC-4, CD-4, and AD-4). The -6 points were adjusted next, one quadrant at a time (C4-6, C5-6, D4-6, D5-6, etc). Next, -5s were adjusted for each quadrant, then -4s and so on, until all points, including catenaries, were coarse adjusted to within 0.254 cm from theoretical parabola.

3.5 FABRICATION OF STEEL DIAGONALS

Before the reflector was installed on the box truss, two sets of equal length graphite diagonals were replaced with unequal lengths to skew the box truss into the offset fed configuration (Fig. 4). Without enough lead time to order new graphite material and to keep costs down, the graphite diagonals were replaced with steel cable and aluminum end fittings. Each set of steel diagonals were required to be two different lengths, 5.675 m for the shorter diagonal and 7.055 m for the longer diagonal. The aluminum end fittings were of similar design as the graphite end fitting they replaced (Fig. 18).

The assembly of the diagonals involved a tool that consisted of two flat aluminum plates each having a vertical 0.318-cm diameter pin protruding from its center. Two tools of this type were fabricated. The plates were positioned on a work table with the pin-to-pin distance being 5.675 m for the shorter set of diagonals and 7.055 m for the longer set. The steel cables were bonded to end fittings on one end only. After grit blast, the end fittings were positioned on the 0.318-cm tool pins. The steel cables were extended through the second set of end fittings and draped over the end of the work table with a 6.8 kg preload weight attached. The second end fittings were bonded in this configuration.

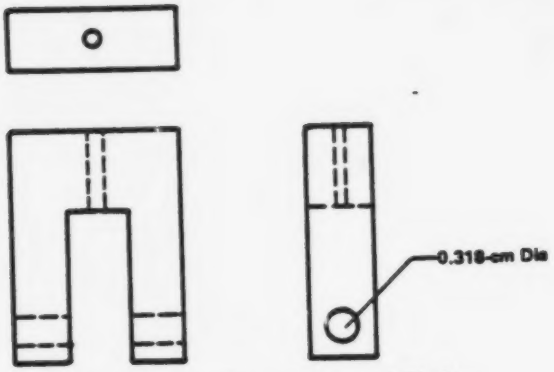

Figure 18 Diagonal Assembly End Fitting

3.6 INSTALLATION ONTO THE BOX TRUSS

Installation was started by attaching two of the mesh standoffs to the truss vertical members after the truss had been set on its side and fully opened in the nonskewed direction. The truss was then slowly deployed in the skewed direction using a hoist and sling to control the truss level for an even deployment. At three-quarters deployment, the two remaining standoffs were attached to the truss vertical members. The deployment was then completed by locking all the box-truss midlink hinges in the deployed position.

At the final stage of deployment, eight of the center tieback cords broke. The probable cause for the breakage was the fact that the graphite truss was not as flexible as the wooden stands used for the mesh/tie system assembly. The wooden stands had allowed the tops of the standoffs to move diagonally 1.27 cm. The graphite truss moved far less, and therefore, caused the entire tie system to rise which over tensioned the graphite tieback cords.

To compensate for the difference in movement, the 3.175-cm aluminum discs at the corners of the mesh were moved diagonally towards the mesh center approximately 0.635 cm. Also, 0.318-cm thick aluminum shims were installed between the outer edge of the graphite corner fittings and the standoffs. This tilted the standoffs toward mesh center. This was still not enough movement, and therefore, the center of the reflector was still under too much tension. This made it necessary to move the four center tie point locations outward by increasing the length of the surface cross cords between the tie points by approximately 1.9 cm for each point (AB-4, BC-4, CD-4, AD-4, Fig. 5). The broken tieback cords were repaired and the truss assembly was turned upright. The four truss corners were leveled in the skewed position with the lower surface tube at 12.54 deg with reference to the floor. Leveling was achieved with a surveyor's transit; the upper standoffs were 0.97-m above the lower standoffs with reference to level.

The theodolites were initialized per the process, which was discussed previously. Approximately 25% of the O-ring stops needed to be replaced because of excessive wear from the coarse adjustment process. The mesh surface tie points were adjusted per the previously discussed procedure with a goal of ± 0.16 cm from the theoretical paraboloid. The adjusting sequence did not follow a circular pattern. Instead, each quadrant was adjusted individually beginning with the tie points at the mesh center and adjusting one arc row at a time working towards the quadrant corner. The quadrant sequence was A, C, D, and B. Interaction between tie points did not appear to be a major factor. The majority of adjusting required the fine adjustment screw versus the coarse adjustment tube.

After each point was set, procedures called for each point to be retargeted by the theodolite system. However, schedule constraints did not permit this verification process. Instead, random tie points were retargeted to verify that the ± 0.16-cm tolerance had been achieved. After verification, the coarse tubes were locked in place with a drop of silicone adhesive. The surface cords were isolated from the 113.4-gram weights by a locking plate that was attached to the standoff top plate. This sandwiched the surface cords between the standoff top plate and the locking plate, which terminated further surface cord movement.

4.0 VERIFICATION OF REFLECTIVE SURFACE

The verification of the reflective surface required that the surface be photogrammetrically measured and the results be analyzed to determine the best-fit paraboloid. From these two operations the actual rms manufacturing error and rms pillowing error were determined.

Since there has always been some concern that deployable tension stabilized mesh reflectors would change shape once they have been set, stowed, then deployed, i.e., repeatability, the verification process was performed twice. First, immediately following the theodolite surface setting, and again, after the reflector had been partially stowed and redeployed. Both sets of results are presented.

4.1 PHOTOGRAMMETRIC MEASUREMENTS

The photogrammetric measurements of the surface were performed by Dick Adams of NASA Langley Research Center at Martin Marietta's facility. To take the photographs, each tie point button had a special reflective target installed on the top. This target was actually installed at the time the tie system was being built. In addition, two sections of mesh bound by tie points were targeted every two inches. These targets were used later to determine the extent of mesh pillowing.

Each target was referenced by a number in order for the photographs to be analyzed by Geodetic Services, Inc of Melbourne, FL. Figures 19 shows the numbering of the tie points and the mesh targets. In addition, twelve of the targets were marked with special target numbers. The targets, along with the location of these targets according to the theodolite measurements, enable Geodetic Services to transform the photographed coordinates of each tie point into the reflector coordinate system. Figure 19 shows the location of the 12 points. Table 4 gives the theodolite coordinates used for the transformation.

Taking the metric camera measurements required that the camera be positioned at six different clock angles around the reflector and remain at a fixed distance ($\sim$4.88-m) above the plane of the reflector. To achieve this requirement, the box truss was laid flat on the floor (Fig. 20). Figure 21 shows the six camera positions relative to the box truss.

The first set of pictures took Dick Adams a day to shoot and develop. After he verified that the photos were good, the truss was set upright and partially stowed. Since the contract schedule did not permit full stowage, the box truss was stowed in both directions about 1 to 1.25 m. This totally relaxed the reflector surface and allowed the surface to realign itself if necessary. Then the truss was redeployed, again laid flat on the floor and the second set of photographs were taken.

PRECEDING PAGE BLANK NOT FILMED

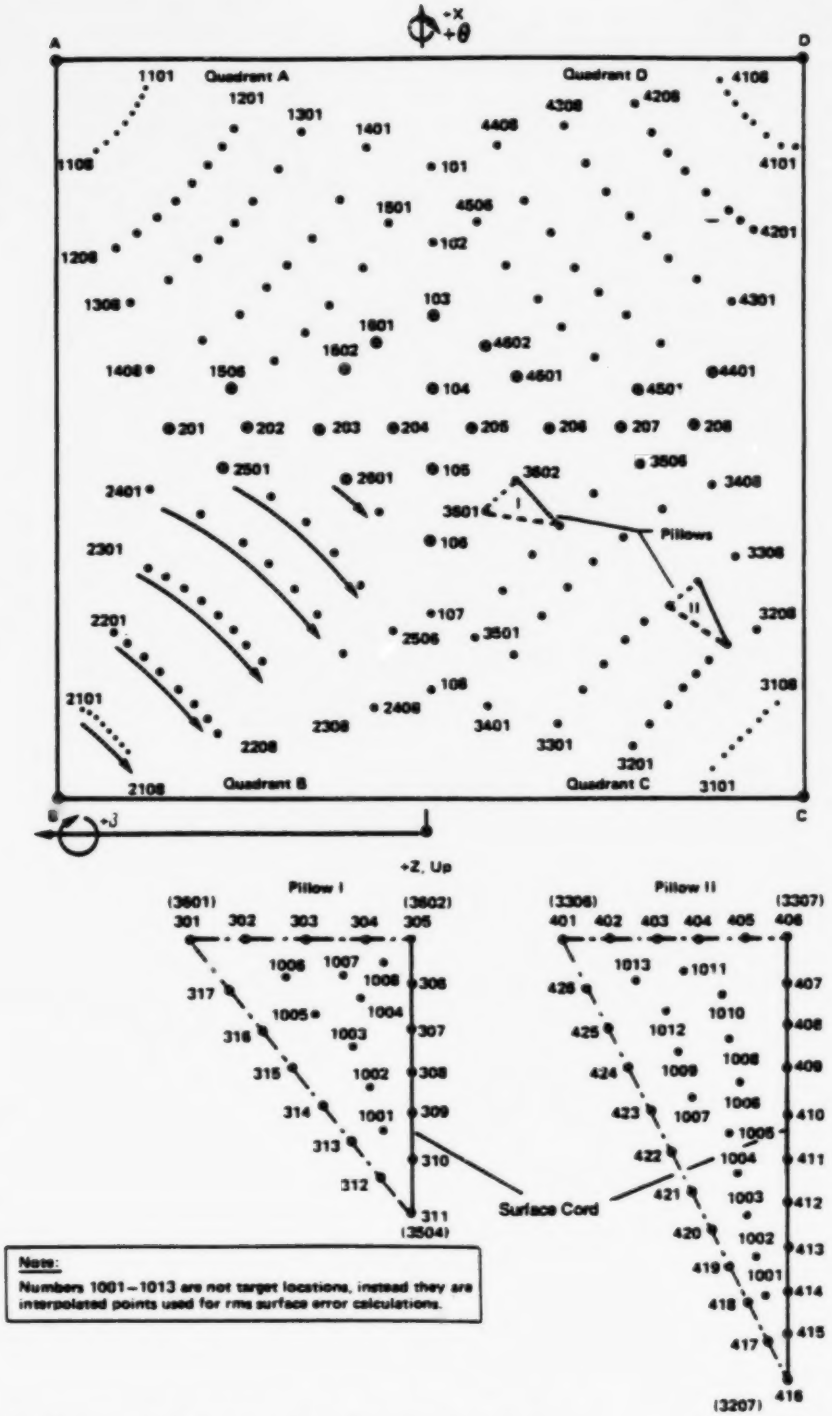

Figure 19 Tie Point and Pillowing Target Numbers

ORIGINAL PAGE IS
OF POOR QUALITY

ORIGINAL PAGE IS
OF POOR QUALITY

Table 4 Baseline Coordinates for Photogrammetric Transformation

Target	Label	X, m	Y, m	Z, m
1	1101	4.916	1.782	1.044
2	1108	4.571	2.117	0.970
3	201	2.836	1.655	0.413
4	2101	1.044	2.145	0.218
5	2108	0.759	1.815	0.149
6	108	1.181	-0.007	0.055
7	3101	0.764	-1.833	0.152
8	3108	1.040	-2.153	0.219
9	208	2.841	-1.669	0.415
10	4101	4.565	-2.113	0.967
11	4108	4.923	-1.785	1.047
12	101	4.430	-0.003	0.749

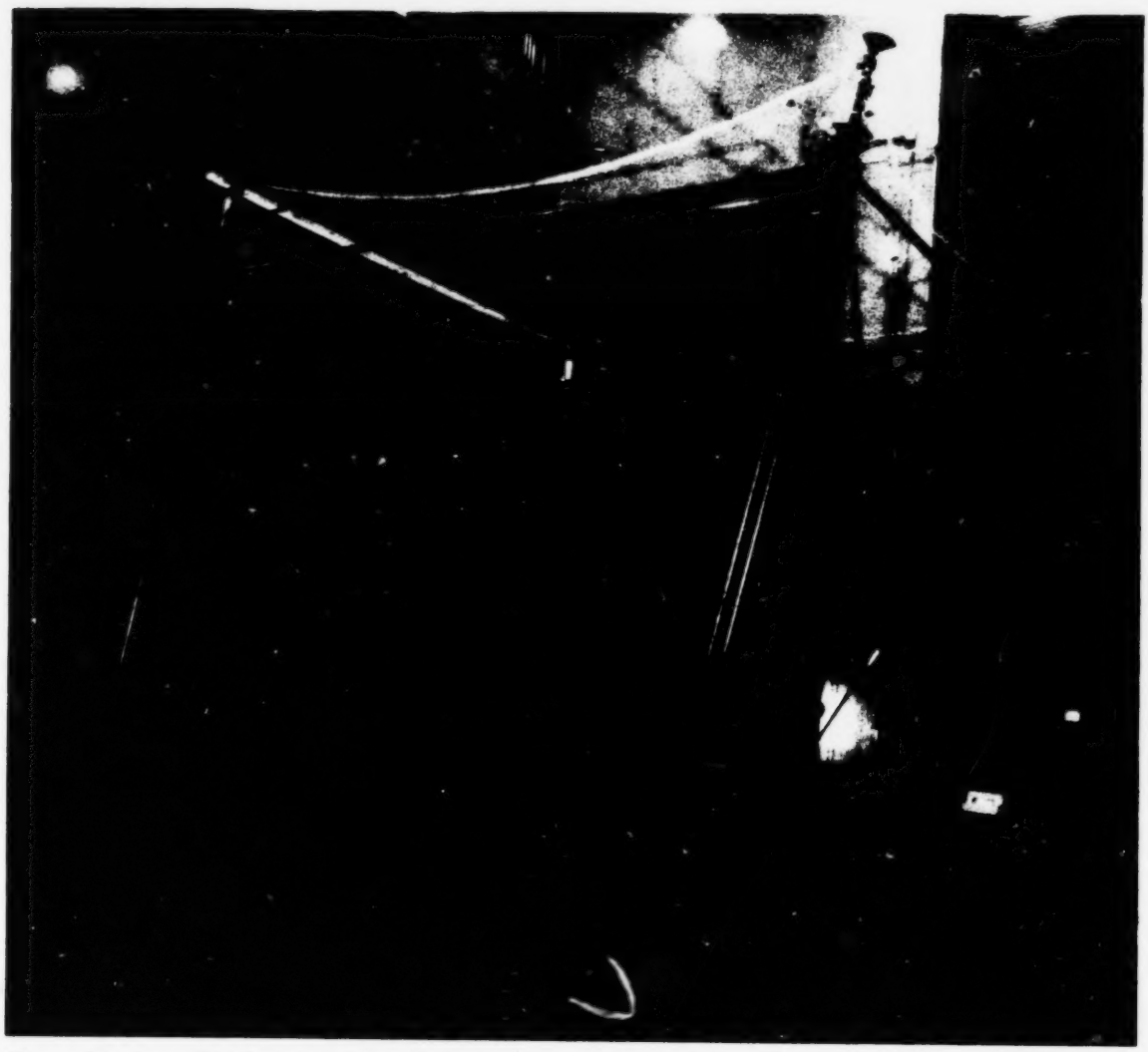

Figure 20 Truss Configuration for Photogrammetric Pictures

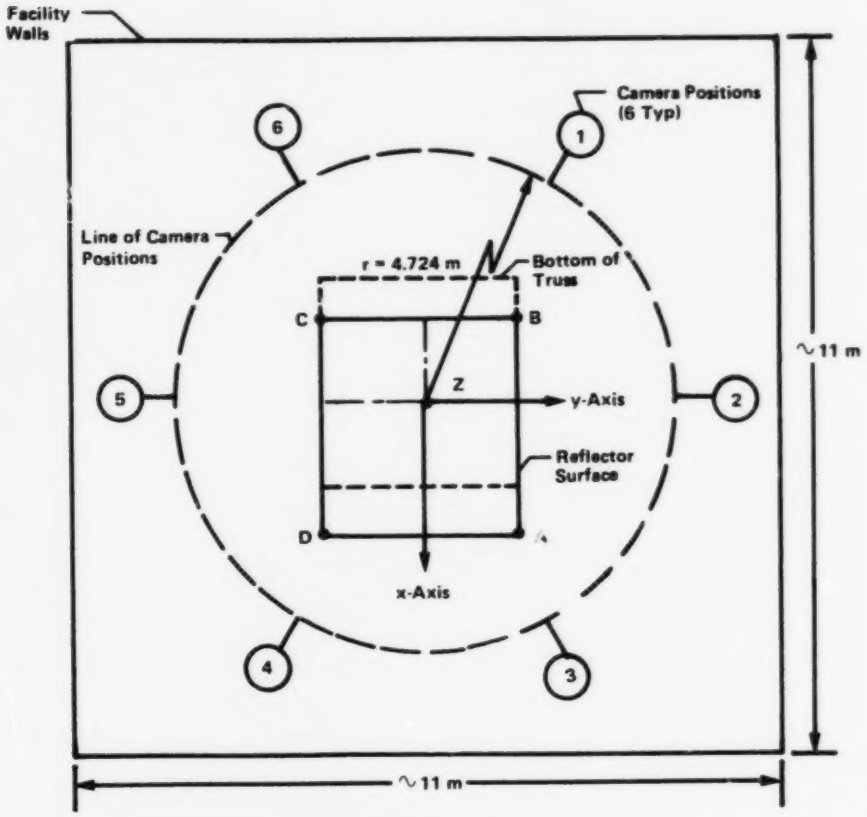

Figure 21 Photogrammetric Camera Positions

From the two metric camera measurements the coordinates of each tie point and mesh pillowing target were determined in a coordinate system best represented by the 12 reference points from the theodolite measurements. The rms standard errors for the metric camera measurements was about 0.025 m in X, Y, and Z with triangulation closures of about 1.4 microns, for both measurement sets. Appendix B contains the coordinates of each target for both sets.

4.2 BEST-FIT ANALYSIS

Using the metric camera coordinates of each tie point, a "best-fit" analysis was performed to isolate the systematic errors in the reflector from the random errors caused by manufacturing and setting. This was achieved by writing a small IBM PC BASIC program, which manipulated the actual tie point coordinates to best-fit perfect surface. The program listing is shown in Appendix C. This program was modeled after the best-fit surface routine (Ref 1).

The manipulations, roll, pitch, change in focal length and surface translations (ΔX, ΔY, and ΔZ), all contribute to systematic errors, e.g., axial defocus, beam scanning, etc (Fig. 22). The difference in the Z- coordinate of the tie point and the corresponding point on the perfect surface is defined as the random error. The best-fit surface is that paraboloidal surface that shows a minimum rms of random surface error (Eq 3).

[3]

$$MANUF_{rms} = \sqrt{\frac{\sum_{i=1}^{N} \left(Z_d - Z_p\right)^2}{N}}$$

where
- Zd = Z- oordinate of tie point
- Zp = Z- coordinate of best-fit surface
- N = total number of tie points, 176
- Manuf rms = rms of random surface error because of manufacturing and setting

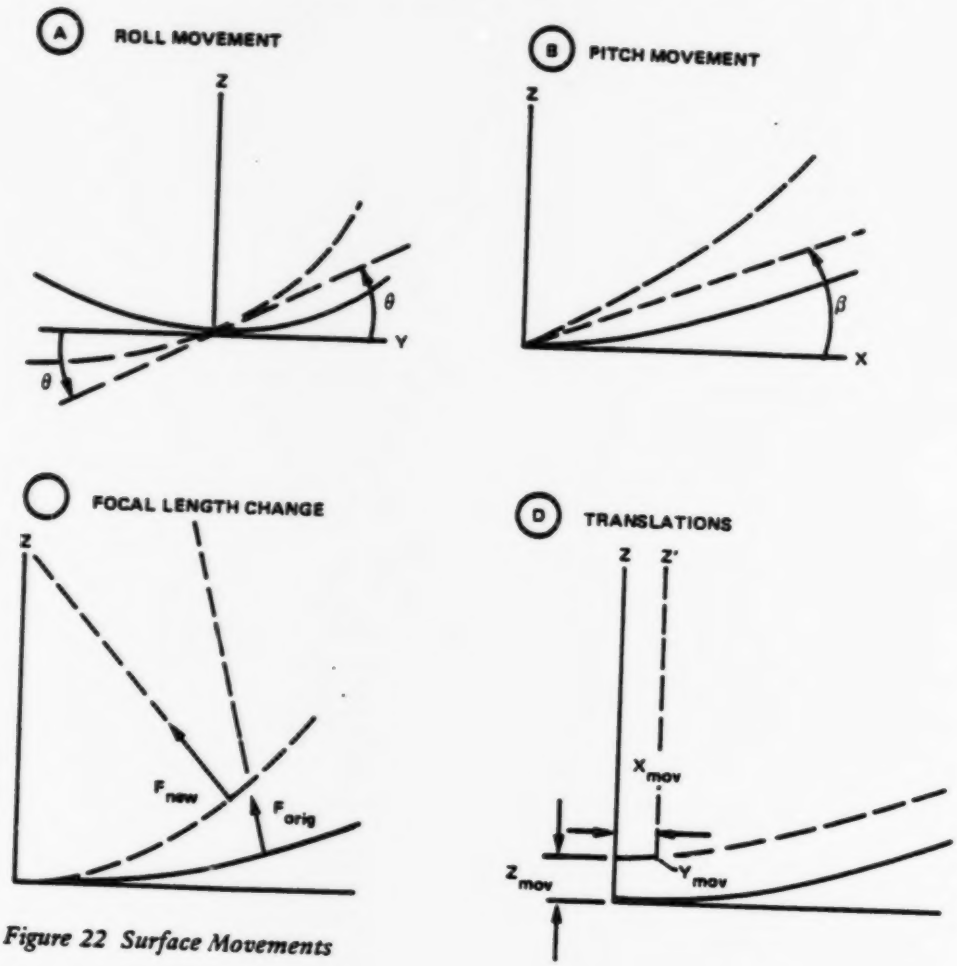

Figure 22 Surface Movements

Before the metric camera measurements could be used in the best-fit computer program, the Z- coordinate had to be revised to account for the tie point button thickness since the targets were placed on the top of the buttons and the mesh was under the buttons. Also, quite a few tieback cords had broken during the installation of the tie system to the mesh and many of the buttons were 3 and 4 (buttons) thick. By measuring a representative number of buttons, a standard tie point, i.e., a surface cord and tieback cord sandwiched between one top button and one bottom button was found to 1.27-m thick. For a tie point with 3 buttons it varied from 1.65 to 1.90-mm thick and for 4 buttons 2.16 to 2.54-mm thick. Therefore, Z- coordinate was reduced by 1.27, 1.78, and 2.29 mm for 2, 3, and 4 button tie points, respectively. Appendix C shows the value used at each point.

During the best-fit analysis of the surface, it became apparent that quadrant C, i.e., tie points 3101 through 3602, was uniformly 2.03-mm lower than all other quadrants. This problem was apparently caused by improper initialization of the theodolite system on the day Quadrant C was adjusted. Therefore, two best-fit analysis cases, one of the whole surface and the other removing all points within Quadrant C, were performed.

The best-fit analysis results showed the following. For the first set of metric camera coordinates, Set 1, i.e, the photos taken immediately following the theodolite surface setting, the minimum rms random surface error was 1.27 mm for the whole surface and 1.02 mm for the partial surface. For the set of coordinates after partial stowage, Set 2, the minimum rms random surface error was 1.25 mm for the whole surface and 1.04 mm for the partial surface. To show repeatability, the second set of metric camera measurements used the identical surface manipulations values as the first. In other words, the same ΔX, ΔY, and ΔZ translations, the same roll and pitch, and the same focal length.

The results show that the surface is extremely stable and repeatability is excellent. However, a more stringent test might require the surface to be fully stowed for some length of time and then redeployed and measured.

Table 5 shows the resulting surface manipulations from performing the best-fit analysis.

Table 5 Best-Fit Surface Manipulations

	Whole Surface	Partial Surface
ΔX, cm	0.0	0.0
ΔY, cm	0.0	0.064
ΔZ, cm	0.157	0.036
F, m	6.538	6.553
Θ Roll, deg	0.0150	0.0003
β Pitch, deg	-0.0010	0.0047

4.3 MESH PILLOWING

Using the metric camera coordinates of the mesh targets, an analysis was performed to determine the rms surface error caused by mesh pillowing.

As with the best-fit analysis, a short BASIC program was written, which took the photographed coordinates and solved for the rms surface error. Appendix D includes a listing of the program.

To isolate pillowing errors from manufacturing errors, the analysis solved for two different flat planes between the three tie points that bound the targeted mesh. For Pillow I, these points were 301, 305, and 311 or 3601, 3602, and 3504, respectively, using the whole surface numbering scheme (Fig. 19). For Pillow II, these points were 401, 406, and 416 or 3306, 3307, and 3207, respectively.

The first flat plane was generated using the X, Y, and Z- coordinates of the three tie points. The second flat plane was generated using only the X and Y coordinates of the tie points and solved for the Z-coordinate using a perfect paraboloid, i.e., a focal length of 6.553 m. Then the distance normal between the first plane and the mesh target point, d_1, was added to the distance normal between the second plane and the perfect paraboloid at the mesh target, d_2. This way the manufacturing errors of the corner tie points were removed. This process is better understood by looking at a two-dimensional illustration (Fig. 23).

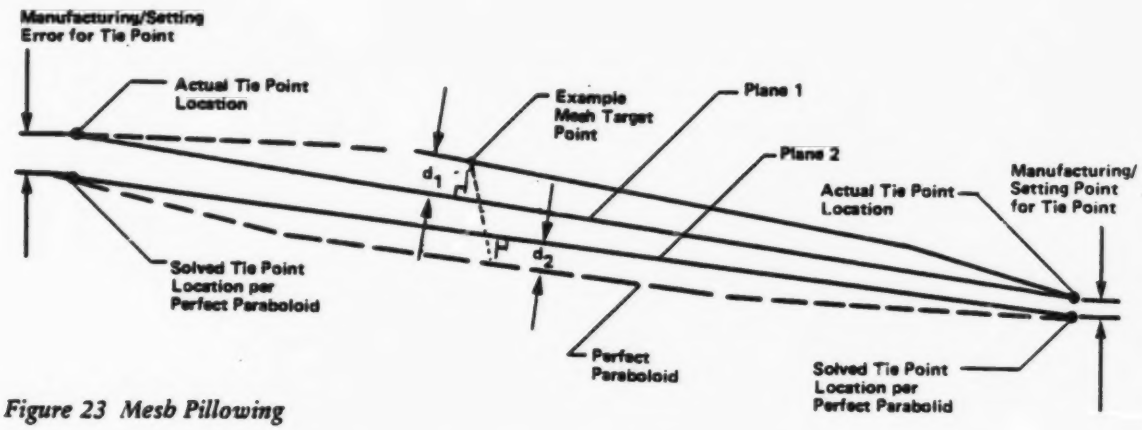

Figure 23 Mesh Pillowing

Once the distance from the paraboloid was determined for each mesh target ($d_1 + d_2$), additional surface points were linearly interpolated so that the mesh pillow could be better represented by a group of points. Figure 19 shows the location of the interpolated points.

Finally, to find the minimum rms surface error because of pillowing, an offset value, d_{ref}, was used for all points. The program iterated on the d_{ref} value until the minimum rms value was found. Equation 4 shows how the rms pillowing error was determined.

[4]
$$Pillow_{rms} = \sqrt{\frac{\sum_{i=1}^{N} M \times \left(d_{TOT} - d_{ref}\right)^2}{N}}$$

where d_{TOT} = distance from paraboloid to mesh, $(d_1 + d_2)$
d_{ref} = offset value used for all points
M = Multipoint factor, 2 for interpolated points, 1 for mesh targets
N = number of total points used to calculate rms
$Pillow_{rms}$ = rms error because of pillowing

Note that within Equation 4 there is a multipoint factor, M, for the interpolated tie points since only half the area bound by tie points was represented by targets.

The analysis results showed that Pillow I has an rms error of 0.043 cm and Pillow II has an rms error of 0.086 cm. Since the two targeted pillow areas represented the upper and lower bounds of mesh pillowing, the two rms values were averaged to determine the rms pillowing error for the whole surface. The average value is 0.066 cm.

4.4 SURFACE AREA SUMMARY

Combining manufacturing errors with pillowing errors results in the following total rms surface error (Table 6).

Table 6 rms Surface Error Summary

	Whole Surface/ Set 1	Partial Surface/ Set 1	Whole Surface/ Set 2	Partial Surface/ Set 2
rms Manufacturing Error, cm	0.127	0.102	0.124	0.104
rms Pillowing Error (ave), cm	0.066	0.066	0.066	0.066
Worst-Case Sum, cm	0.193	0.168	0.191	0.170
rss of rms Errors, cm	0.142	0.122	0.140	0.124
Average of Worst-Case/ rss, cm	0.168	0.145	0.166	0.147

Since the actual rms surface error will be somewhere in between the worst-case sum of the errors and the rss of the errors, an average total surface error was determined. For the whole surface, the average

rms surface error of 0.168 cm represents an achieved surface accuracy of 1/18 of a wavelength of 10 GHz. For the partial surface, the total surface error of 0.145 cm represents an achieved surface accuracy of 1/21 of a wavelength.

Although the goal of 1/25 of a wavelength was not achieved, as a first effort for integrating a mesh reflector to a box truss and considering the configuration was changed from centered to offset midway through the effort, the achieved surface accuracy of 1/18 of a wavelength is a remarkable result. It also shows that by going back and readjusting the surface one additional time, the 1/25 of a wavelength goal can be achieved.

5.0 COMPARISON OF RESULTS WITH ANALYTICAL PREDICTIONS

The schedule did not permit the loads in the tie system to be measured so that they could be compared with the analytical predictions using software (Ref 1). However, two major assumptions within the software could be verified, i.e., mesh pillowing and manufacturing rms surface errors.

5.1 MESH PILLOWING EQUATION

In Reference 1 we presented the equation shown below, Equation 5, for predicting the rms surface error because of pillowing for box truss antenna systems which use the direct tieback tie system.

$$[5] \quad \text{rms (pillow)} = \frac{0.05 \times TS^2}{F}$$

where TS = Radial Tie Spacing, m
F = Antenna Focal Length, m and
rms (pillow) = rms surface error caused by pillowing, m

The equation assumed a square tie point pattern. However, the direct tieback tie system does not produce a square tie point pattern, therefore, TS^2 should be equal to the area of mesh bound by the tie points. For a square pattern tie system, the tie spacing square and TS^2 are equal. Using this correction and comparing it to the measured pillow shapes results in Table 7.

Table 7 Verification of Pillowing Error Equation

Pillow I

Mesh Area Bound by Tie Points = 18.8 cm x 30.5 cm = 573.4 cm² (0.057 m²)

Analytically Predicted rms Error Caused by Pillowing = $\frac{0.05\ (0.057)}{6.5532}$ = 4.349 x 10^{-4}m (0.043 cm)

Measured rms Error
Caused by Pillowing = 0.043 cm
% Difference = 0.0

Pillow II

Mesh Area Bound by Tie Points = 20.3 cm x 50.8 cm = 1031.24 cm² (0.103 m²)

Analytically Predicted rms Error Caused by Pillowing = $\frac{0.05\ (0.103)}{6.5532}$ = 7.859 x 10^{-4}m (0.079 cm)

Measured rms Error
Caused by Pillowing = 0.088 cm
% Difference = 8.1

PRECEDING PAGE BLANK NOT FILMED

As shown in Table 7, the equation will predict the rms surface error caused by pillowing within 10% or less.

5.2 MANUFACTURING EQUATION

Along with the mesh pillowing equation, the equation shown below, Equation 6 was presented in Reference 1 for predicting the rms surface error because of a defined manufacturing tolerance.

[6] $rms(manuf) = MT/3$

where MT = manufacturing tolerance, and
rms(manuf) = rms surface error caused by manufacturing errors

Although this task attempted to achieve a manufacturing tolerance of $\pm$ 0.16 cm, this was not the case. Instead, the best-fit analysis showed the following achieved manufacturing tolerances and rms surface error for each case analyzed (Table 8). Included in the table is the predicted rms error using Equation 6.

Table 8 Verification of Manufacturing Error Equation

	Manuf Tolerance, cm	Actual rms Error, cm	Predicted rms Error, cm	% Difference
Whole Surface/Set 1	0.432	0.127	0.144	13.3
Partial Surface/Set 1	0.343	0.102	0.114	12.6
Whole Surface/Set 2	0.419	0.124	0.140	12.2
Partial Surface/Set 2	0.356	0.104	0.118	13.8

As shown in Table 8, the manufacturing error equation will predict the rms surface error conservatively, and within 15% or less.

6.0 SUMMARY AND RECOMMENDATIONS

Task 3 results have shown that the box truss is a viable candidate for supporting lightweight mesh reflectors. The 4.572-m, 1.5 F/D, offset fed reflector built under this task achieved a surface accuracy of 1/18 of a wavelength at 10 GHz. This was accomplished by using 3000 tow Celion graphite cords to produce a direct tieback tie system consisting of 176 tie points. Adjustment fittings at each corner allow each tie point to be adjusted.

Although this reflector uses a single box truss cube, multiple bay box truss structures could use the same technology to produce large reflective surfaces. This means each box section of mesh could be manufactured separately, drastically reducing the cost and complexity over other large reflector concepts. The process for sewing the mesh sections together was also included in this study.

Task 3 has solved many of the problems associated with designing and building box truss mesh reflectors. It has also produced a number of recommendations to follow for continued efforts. The following will reduce the cost and complexity, as well as improve the stability and accuracy of installing mesh reflectors on box truss structures.

1) During the fabrication and installation of this reflector, over 24 tieback cords were broken either at the tie point or at the adjustment fitting. This was because of the sensitivity of the Celion graphite cord to handling and bending. Consider using either Kevlar cord, quartz cord or if the thermal and stiffness requirements dictate, use Celion cord with an outer nylon wrapping. For R&D work, Kevlar seems the most durable and coatings have been developed to reduce the ultraviolet degradation effects.

2) The present design bonded the ends of the catenaries in place on the stretching table. Later, during the installation and coarse setting they were pulled down into shape, thereby increasing the tension in the cords. Instead, the catenaries should be installed on the stretching table, but not bonded. When the mesh is installed on the standoffs and the catenaries are pulled into shape, the catenary can then be tensioned by hanging weights and bonded. This process provides the flexibility of adjusting the catenary depth and the tension level if required without having to replace the catenary cords.

3) An improvement can be made to the tieback cord adjustment hardware. Presently, the graphite cord is bonded directly to the fine adjustment allen screw that is located at the end of the coarse adjustment tube (Fig. 11). The coarse adjustment tube cannot be turned in a threaded fixture for adjustment; this would cause the tieback cords to twist excessively and cause premature breakage. Therefore, the tube is moved in or out of the adjustment fitting, which does not twist the graphite cord.

A metal cable should be bonded to the fine adjustment allen screw and extend outward from the end of the coarse tube. A swivel should be attached to the end of the wire to which the tieback cord will be attached. This allows the coarse adjustment tube to be threaded into the adjustment fitting and would greatly increase the ease of coarse adjustment.

4) A redesign of the adjustment fitting is desirable to simplify the physical arrangement of the adjustment hardware. The tieback lines-of-action converge at the center of the square tube at the base of the standoff. When all the coarse adjustment tubes (48 each) are installed into the adjustment angle fitting along their line-of-action, the ends of the adjustment tubes are close to touching and access to some of the fine adjustment allen screws is very difficult.

   If the adjustment hardware is modified per Item 3 above, it is possible to relocate the adjustment angle fitting to the lower outside (opposing) corner of the cube corner fitting. This provides access to both the coarse adjustment screw and fine adjustment screw from the outside of the adjustment fitting angle. The angle presently used for installing the adjustment hardware would remain to guide the tieback cords and an eyelet or multiple eyelets would be located at the line-of-action point of intersection. The placement of the adjustment hardware in the new adjustment angle could be along horizontal rows of threaded holes and therefore spacing between adjustment screws could be smaller allowing for many more tieback cords to be added to the design. The metal cable attached to a tieback would be routed through the top inside angle through the eyelet and into the coarse adjustment screw on the bottom outside angle. Figure 24 illustrates this concept. Note that the tieback cords pass through what is presently the base plate of the cube corner fitting. Therefore, the base plate of the fitting would have to be modified with an access hole.

   This design would make it possible to adjust the surface for multibay box truss antennas at locations where one standoff is used by up to four different box truss cabes. If the metal cables should prove too bulky through the eyelet, an alternative would be to use Kevlar which will tolerate the wear of the cord through the eyelet.

5) Finally, the single bay reflector was adjusted for a parabolic shape while it was set up on the wooden stands (Fig. 17). Although this greatly eased the assembly process, i.e., not having to work 4.8 meters in the air, it caused some tieback cords to fail since the stands did not precisely duplicate the truss stiffness. That is, when the tensioned tie system was later installed on the box truss and the box truss did not deflect as much as the wooden stands, the tieback cords became overloaded and failed. In the

future, the floor stands should be used solely for installing the tie system onto the mesh surface. At this point the reflector should be installed on the box truss and surface set to the paraboloidal shape. This means either scaffolding must be used or the box truss must be lowered into a pit so that access to the adjustment fittings requires minimal effort.

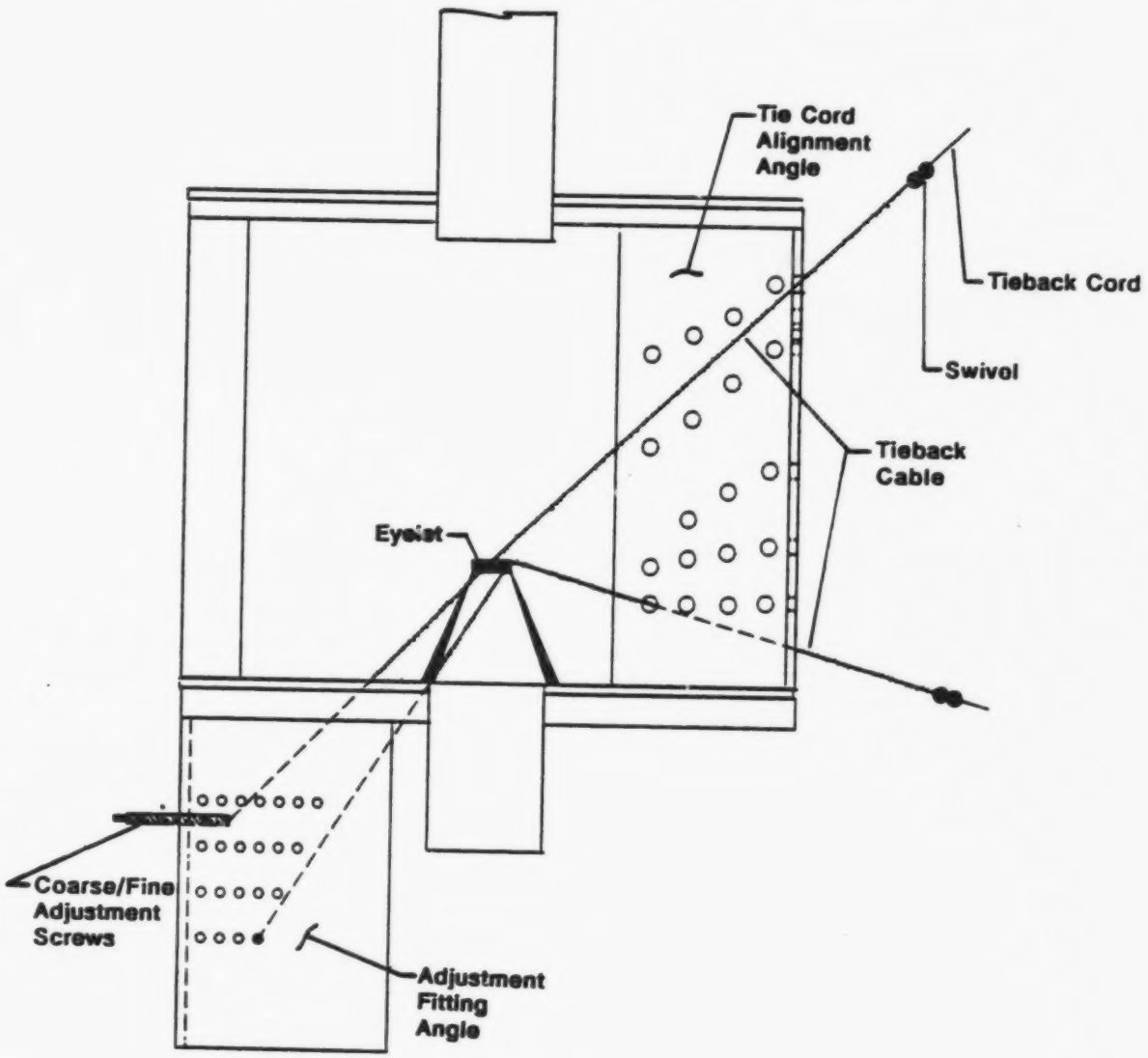

Figure 24 Redesigned Attachment Fitting

7.0 REFERENCE

1. E. E. Bachtell et al.: "Box Truss Analysis and Technology Development, Task 1--Mesh Analysis and Control." NASA CR-172570, August 1985.

PRECEDING PAGE BLANK NOT FILMED

APPENDIX A

The following coordinates define the location of each tie point on the mesh reflector. The coordinates where hand generated by translating the center-fed configuration defined in Section 2.1, page 9. The translation consisted of a 2.8956-m translation along the X-axis and a 12.2368-degree rotation about the Y-axis.

TIE POINT COORDINATES IN METERS

TIE POINT	X,m	Y,m	Z,m
A	5.0752	2.2860	1.1820
B	0.6096	2.2860	0.2135
C	0.6096	-2.2860	0.2135
D	5.0752	-2.2860	1.1820
AB-1	2.8298	1.6537	0.4098
AB-2	2.8298	1.1472	0.3557
AB-3	2.8298	0.6398	0.3211
AB-4	2.8298	0.1319	0.3062
BC-1	1.2136	0.0	0.0562
BC-2	1.7087	0.0	0.1114
BC-3	2.2045	0.0	0.1854
BC-4	2.7009	0.0	0.2783
CD-1	2.8298	-1.6537	0.4098
CD-2	2.8298	-1.1472	0.3557
CD-3	2.8298	-0.6398	0.3211
CD-4	2.8298	-0.1319	0.3062
AD-1	4.4460	0.0	0.7541
AD-2	3.9510	0.0	0.5955
AD-3	3.4551	0.0	0.4554
AD-4	2.9588	0.0	0.3340
A9-1	4.9328	1.8011	1.0520
A9-2	4.8013	1.3146	0.9454
A9-3	4.6694	0.8267	0.8579
A9-4	4.5577	0.4134	0.7990
A10-1	4.8451	1.8366	1.0242
A10-2	4.6255	1.3855	0.8894
A10-3	4.4052	0.9330	0.7735
A10-4	4.1844	0.4794	0.6767
A10-5	4.0677	0.2397	0.6334
A11-1	4.7775	1.8790	1.0054
A11-2	4.4899	1.4704	0.8515
A11-3	4.2014	1.0604	0.7163
A11-4	3.9121	0.6494	0.5999
A11-5	3.6836	0.3247	0.5217
A12-1	4.7278	1.9211	0.9935
A12-2	4.3905	1.5547	0.8276
A12-3	4.0520	1.1871	0.6801
A12-4	3.7126	0.8186	0.5514
A12-5	3.3726	0.4494	0.4416
A12-6	3.1657	0.2247	0.3842
A13-1	4.7073	1.9422	0.9892
A13-2	4.3492	1.5969	0.8189
A13-3	3.9900	1.2506	0.6670
A13-4	3.6298	0.9033	0.5338
A13-5	3.2690	0.5554	0.4194
A13-6	3.0494	0.3437	0.3593
A14-1	4.6661	1.9929	0.9821
A14-2	4.2668	1.6987	0.8046
A14-3	3.8661	1.4034	0.6453
A14-4	3.4645	1.1075	0.5047
A14-5	3.1472	0.8737	0.4070
A15-1	4.6247	2.0621	0.9782
A15-2	4.1838	1.8374	0.7966
A15-3	3.7416	1.6120	0.6332
A15-4	3.2983	1.3860	0.4883
A15-5	3.0641	1.2666	0.4194
A16-1	4.5900	2.1519	0.9804
A16-2	4.1145	2.0173	0.8011
A16-3	3.6377	1.8824	0.6400
A16-4	3.2338	1.7681	0.5182
B1-1	0.7268	0.1801	0.1439
B1-2	0.8583	1.3146	0.0940
B1-3	0.9902	0.8267	0.0635
B1-4	1.1019	0.4134	0.0528
B2-1	0.8145	1.8366	0.1540
B2-2	1.0342	1.3855	0.1140
B2-3	1.2545	0.9330	0.0932
B2-4	1.4753	0.4794	0.0918
B2-5	1.5920	0.2397	0.0989
B3-1	0.8822	1.8790	0.1644
B3-2	1.1698	1.4704	0.1347
B3-3	1.4583	1.0604	0.1240
B3-4	1.7475	0.6494	0.1326
B3-5	1.9760	0.3247	0.1530
B4-1	0.9318	1.9211	0.1739
B4-2	1.2692	1.5547	0.1537
B4-3	1.6077	1.1870	0.1524
B4-4	1.9470	0.8186	0.1702
B4-5	2.2870	0.4494	0.2072
B4-6	2.4940	0.2247	0.2392
B5-1	0.9524	1.9422	0.1785
B5-2	1.3104	1.5969	1.6280
B5-3	1.6696	1.2506	1.6600
B5-4	2.0298	0.9033	0.1883
B5-5	2.3906	0.5554	0.2298
B5-6	2.6102	0.3437	0.2644
B6-1	0.9935	1.9930	0.1892
B6-2	1.3929	1.6987	0.1841
B6-3	1.7935	1.4034	0.1978
B6-4	2.1952	1.1075	0.2306
B6-5	2.5125	0.8737	0.2699
B7-1	1.0350	2.0621	0.2031
B7-2	1.4758	2.8374	0.2119
B7-3	1.9180	1.6120	0.2395
B7-4	2.3613	1.3860	0.2860
B7-5	2.5956	1.2666	0.3182
B8-1	1.0696	2.1519	0.2203
B8-2	1.5451	2.0173	0.2463
B8-3	2.0219	1.8824	0.2911
B8-4	2.4259	1.7681	0.3438

TIE POINT COORDINATES IN METERS

TIE POINT	X,m	Y,m	Z,m	TIE POINT	X,m	Y,m	Z,m
C1-1	0.7268	-0.1801	0.1439	D9-1	4.9328	-1.8011	1.0520
C1-2	0.8583	-1.3146	0.0940	D9-2	4.8013	-1.3146	0.9454
C1-3	0.9902	-0.8267	0.0635	D9-3	4.6694	-0.8267	0.8579
C1-4	1.1019	-0.4134	0.0528	D9-4	4.5577	-0.4134	0.7990
C2-1	0.8145	-1.8366	0.1540	D10-1	4.8451	-1.8366	1.0242
C2-2	1.0342	-1.3855	0.1140	D10-2	4.6255	-1.3855	0.8894
C2-3	1.2545	-0.9330	0.0932	D10-3	4.4052	-0.9330	0.7735
C2-4	1.4753	-0.4794	0.0918	D10-4	4.1844	-0.4794	0.6767
C2-5	1.5920	-0.2397	0.0989	D10-5	4.0677	-0.2397	0.6334
C3-1	0.8822	-1.8790	0.1644	D11-1	4.7775	-1.8790	1.0054
C3-2	1.1698	-1.4704	0.1347	D11-2	4.4899	-1.4704	0.8515
C3-3	1.4583	-1.0604	0.1240	D11-3	4.2014	-1.0604	0.7163
C3-4	1.7475	-0.6494	0.1326	D11-4	3.9121	-0.6494	0.5999
C3-5	1.9760	-0.3247	0.1530	D11-5	3.6836	-0.3247	0.5217
C4-1	0.9318	-1.9211	0.1739	D12-1	4.7278	-1.9211	0.9935
C4-2	1.2692	-1.5547	0.1537	D12-2	4.3905	-1.5547	0.8276
C4-3	1.6077	-1.1870	0.1524	D12-3	4.0520	-1.1871	0.6801
C4-4	1.9470	-0.8186	0.1702	D12-4	3.7126	-0.8186	0.5514
C4-5	2.2870	-0.4494	0.2072	D12-5	3.3726	-0.4494	0.4416
C4-6	2.4940	-0.2247	0.2392	D12-6	3.1657	-0.2247	0.3842
C5-1	0.9524	-1.9422	0.1785	D13-1	4.7073	-1.9422	0.9892
C5-2	1.3104	-1.5969	1.6280	D13-2	4.3492	-1.5969	0.8189
C5-3	1.6696	-1.2506	1.6600	D13-3	3.9900	-1.2506	0.6670
C5-4	2.0298	-0.9033	0.1883	D13-4	3.6298	-0.9033	0.5338
C5-5	2.3906	-0.5554	0.2298	D13-5	3.2690	-0.5554	0.4194
C5-6	2.6102	-0.3437	0.2644	D13-6	3.0494	-0.3437	0.3593
C6-1	0.9935	-1.9930	0.1892	D14-1	4.6661	-1.9929	0.9821
C6-2	1.3929	-1.6987	0.1841	D14-2	4.2668	-1.6987	0.8046
C6-3	1.7935	-1.4034	0.1978	D14-3	3.8661	-1.4034	0.6453
C6-4	2.1952	-1.1075	0.2306	D14-4	3.4645	-1.1075	0.5047
C6-5	2.5125	-0.8737	0.2699	D14-5	3.1472	-0.8737	0.4070
C7-1	1.0350	-2.0621	0.2031	D15-1	4.6247	-2.0621	0.9782
C7-2	1.4758	-2.8374	0.2119	D15-2	4.1838	-1.8374	0.7966
C7-3	1.9180	-1.6120	0.2395	D15-3	3.7416	-1.6120	0.6332
C7-4	2.3613	-1.3860	0.2860	D15-4	3.2983	-1.3860	0.4883
C7-5	2.5956	-1.2666	0.3182	D15-5	3.0641	-1.2666	0.4194
C8-1	1.0696	-2.1519	0.2203	D16-1	4.5900	-2.1519	0.9804
C8-2	1.5451	-2.0173	0.2463	D16-2	4.1145	-2.0173	0.8011
C8-3	2.0219	-1.8824	0.2911	D16-3	3.6377	-1.8824	0.6400
C8-4	2.4259	-1.7681	0.3438	D16-4	3.2338	-1.7681	0.5182

Note: Tie Point labeling is based on the standoff letter, the radial surface cord number and a dash number, i.e., tie point C5-3 is the third tie point out from the 'C' standoff along the number 5 radial surface cord. For the tie points along the surface cross cords, the label is based on the standoff letters and a dash number, i.e., AD-2 is the second tie point on the surface cross cord between standoffs 'A' and 'D'.

APPENDIX B

Coordinates of Target Points for Set 1 of Metric Camera Measurements

Coordinates shown in inches

Target #	X	Y	Z	Button Thk.	Z corrected
101	174.5767	-0.0849	29.5592	0.0700	29.4892
102	155.6399	-0.0218	23.6123	0.0500	23.5623
103	136.3680	-0.2272	18.1078	0.0700	18.0378
104	116.9635	-0.4078	13.4705	0.0700	13.4005
105	105.3839	-0.2522	10.8110	0.0700	10.7410
106	85.7402	0.1377	7.1285	0.0700	7.0585
107	65.7344	-0.2518	4.2018	0.0700	4.1318
108	46.1923	-0.2570	2.1364	0.0700	2.0664
201	111.7774	65.1213	16.3123	0.0500	16.2623
202	111.4182	45.3427	14.0399	0.0500	13.9899
203	111.5721	25.4650	12.7729	0.0700	12.7029
204	111.1280	5.6150	12.1745	0.0700	12.1045
205	111.0440	-6.1907	12.1071	0.0700	12.0371
206	111.3583	-26.1304	12.6630	0.0500	12.6130
207	111.4585	-46.1052	14.0316	0.0500	13.9816
208	111.7537	-65.6485	16.2997	0.0500	16.2497
301	97.4224	-8.9365	9.1682	0.0900	9.0782
302	98.6564	-10.0846	9.4053	0.0000	9.4053
303	99.8601	-11.4735	9.7068	0.0000	9.7068
304	101.1683	-12.8488	9.9978	0.0000	9.9978
305	102.3508	-14.3144	10.2949	0.0900	10.2049
306	100.9648	-15.6418	10.0375	0.0000	10.0375
307	99.5466	-16.9990	9.8086	0.0000	9.8086
308	98.1149	-18.3449	9.5769	0.0000	9.5769
309	96.6949	-19.7945	9.3594	0.0000	9.3594
310	95.2242	-21.2189	9.1177	0.0000	9.1177
311	93.6654	-22.6603	8.9018	0.0500	8.8518
312	94.1246	-20.6130	8.8876	0.0000	8.8876
313	94.7198	-18.6885	8.9476	0.0000	8.9476
314	95.2228	-16.8052	8.9753	0.0000	8.9753
315	95.7076	-14.7426	9.0046	0.0000	9.0046
316	96.2214	-12.9111	9.0446	0.0000	9.0446
317	96.7810	-10.8633	9.0766	0.0000	9.0766
401	69.8125	-55.9920	7.7258	0.0500	7.6758
402	70.8117	-57.5998	8.0343	0.0000	8.0343
403	71.8563	-59.2457	8.3809	0.0000	8.3809
404	72.8589	-60.8685	8.7069	0.0000	8.7069
405	73.9062	-62.5257	9.0352	0.0000	9.0352
406	74.9145	-64.2212	9.3796	0.0500	9.3296
407	73.2890	-65.1566	9.2597	0.0000	9.2597
408	71.4937	-66.0965	9.1572	0.0000	9.1572
409	69.6656	-66.9724	9.0394	0.0000	9.0394
410	67.9156	-67.9061	8.9434	0.0000	8.9434
411	65.9943	-68.8105	8.8206	0.0000	8.8206
412	64.2557	-69.7271	8.7176	0.0000	8.7176
413	62.4960	-70.5873	8.6113	0.0000	8.6113
414	60.6350	-71.5437	8.5059	0.0000	8.5059
415	58.8515	-72.4576	8.3918	0.0000	8.3918
416	57.0763	-73.2636	8.3309	0.0700	8.2609
417	58.1689	-71.4972	8.1875	0.0000	8.1875
418	59.3320	-69.9030	8.1206	0.0000	8.1206
419	60.4152	-68.2033	8.0332	0.0000	8.0332
420	61.6712	-66.5807	7.9743	0.0000	7.9743
421	62.7548	-65.1380	7.9251	0.0000	7.9251
422	64.0453	-63.3957	7.8673	0.0000	7.8673

423	65.2702	-61.8297	7.8115	0.0000	7.8115
424	66.4150	-60.3084	7.7769	0.0000	7.7769
425	67.4998	-58.7030	7.7226	0.0000	7.7226
426	68.7570	-57.0959	7.6823	0.0000	7.6823
1101	193.4932	70.1454	41.0864	0.0500	41.0364
1102	190.0705	71.4708	40.0305	0.0500	39.9805
1103	187.1378	72.8225	39.1319	0.0500	39.0819
1104	185.2847	74.1967	38.6618	0.0500	38.6118
1105	184.0883	74.9196	38.3411	0.0900	38.2511
1106	182.3985	77.2971	38.1135	0.0900	38.0235
1107	180.7293	79.7782	37.8708	0.0500	37.8208
1108	179.8449	83.2785	38.1264	0.0500	38.0764
1201	188.4927	51.1894	37.0552	0.0500	37.0052
1202	181.9847	53.9113	34.9745	0.0500	34.9245
1203	176.4385	56.9213	33.3742	0.0900	33.2842
1204	172.4823	60.2516	32.3959	0.0500	32.3459
1205	170.5274	61.7095	31.9191	0.0900	31.8291
1206	167.1863	66.2441	31.4044	0.0900	31.3144
1207	164.0406	71.1783	31.0734	0.0900	30.9834
1208	161.6957	78.4058	31.3688	0.0500	31.3188
1301	183.2253	32.2751	33.6631	0.0900	33.5731
1302	173.5559	36.2483	30.5202	0.0900	30.4302
1303	165.1652	41.1127	28.1583	0.0900	28.0683
1304	159.4310	46.1458	26.8054	0.0900	26.7154
1305	156.6585	48.4936	26.1642	0.0900	26.0742
1306	151.9946	54.6319	25.3162	0.0500	25.2662
1307	147.0394	62.6210	24.8325	0.0500	24.7825
1308	143.3535	73.3788	25.2219	0.0500	25.1719
1401	178.7323	16.1132	31.2847	0.0500	31.2347
1402	164.8184	18.7651	26.7197	0.0500	26.6697
1403	153.9915	25.3033	23.6651	0.0500	23.6151
1404	146.2951	31.9295	21.7991	0.0500	21.7491
1405	142.8212	35.0229	21.0407	0.0900	20.9507
1406	136.5846	43.2229	19.9674	0.0500	19.9174
1407	129.9898	53.8496	19.3475	0.0900	19.2575
1408	127.6505	69.1274	20.4931	0.0500	20.4431
1501	160.2233	9.3601	25.0508	0.0500	25.0008
1502	145.0508	12.6303	20.6114	0.0500	20.5614
1503	133.0706	17.6290	17.5720	0.0500	17.5220
1504	128.7877	21.5795	16.6115	0.0500	16.5615
1505	124.1851	34.1906	16.1225	0.0500	16.0725
1506	120.8110	49.4802	16.5832	0.0500	16.5332
1601	124.9363	8.9021	15.3279	0.0900	15.2379
1602	120.0979	13.4703	14.2761	0.0500	14.2261
2101	41.0954	84.4063	8.5835	0.0500	8.5335
2102	39.2844	81.7885	8.0541	0.0900	7.9641
2103	37.7449	79.7257	7.5886	0.0900	7.4986
2104	36.3673	77.7158	7.1860	0.0500	7.1360
2105	35.8127	76.9654	7.0008	0.0500	6.9508
2106	34.2347	75.6460	6.7400	0.0500	6.6900
2107	32.1110	73.3690	6.2922	0.0500	6.2422
2108	29.8886	71.4858	5.8521	0.0500	5.8021
2201	60.3751	79.1729	9.7049	0.0500	9.6549
2202	57.2637	73.1150	8.4038	0.0500	8.3538
2203	53.9547	68.0504	7.4697	0.0900	7.3797
2204	50.9789	64.1042	6.5812	0.0500	6.5312
2205	49.4009	62.3338	6.1737	0.0500	6.1237
2206	45.5922	59.2640	5.4587	0.0500	5.4087
2207	40.7204	55.4286	4.6075	0.0900	4.5175
2208	35.0044	52.2432	3.9073	0.0500	3.8573

2301	79.4588	73.6942	11.4132	0.0500	11.3632
2302	75.0242	63.8325	9.4215	0.0900	9.3315
2303	70.0386	56.1066	7.8060	0.0500	7.7560
2304	65.2817	50.0270	6.5766	0.0500	6.5266
2305	62.9373	47.6173	6.0801	0.0500	6.0301
2306	57.1129	42.8124	4.9388	0.0500	4.8888
2307	49.3765	37.3047	3.7584	0.0500	3.7084
2308	39.5886	32.8892	2.5356	0.0500	2.4856
2401	95.6987	69.1337	13.4968	0.0500	13.4468
2402	92.5918	54.6085	11.2051	0.0900	11.1151
2403	85.8451	44.0460	9.0728	0.0500	9.0228
2404	79.4191	35.9707	7.4310	0.0900	7.3410
2405	76.2924	32.7320	6.6702	0.0500	6.6202
2406	68.3794	26.4192	5.2642	0.0500	5.2142
2407	57.6833	19.2307	3.6183	0.0500	3.5683
2408	43.2259	16.3175	2.1082	0.0500	2.0582
2501	101.9652	49.8853	12.4429	0.0500	12.3929
2502	98.3813	34.5278	10.6467	0.0900	10.5567
2503	93.7261	22.1672	9.0025	0.0500	8.9525
2504	89.6228	17.9903	8.1320	0.0500	8.0820
2505	77.1976	13.3113	5.9504	0.0500	5.9004
2506	61.9989	9.5955	3.8126	0.0500	3.7626
2601	102.3279	13.7740	10.3613	0.0500	10.3113
2602	97.6269	8.9271	9.3622	0.0900	9.2722
3101	30.1247	-72.0489	5.8817	0.0500	5.8317
3102	32.2623	-73.7029	6.3146	0.0500	6.2646
3103	34.4242	-75.6635	6.7377	0.0500	6.6877
3104	36.0300	-77.3497	7.1066	0.0900	7.0166
3105	36.5052	-78.3762	7.3176	0.0900	7.2276
3106	37.8009	-80.0123	7.6564	0.0900	7.5664
3107	39.1940	-82.2219	8.1010	0.0700	8.0310
3108	41.0236	-84.7568	8.6962	0.0500	8.6462
3201	34.6846	-52.7204	3.8489	0.0500	3.7989
3202	40.8645	-55.7496	4.6204	0.0500	4.5704
3203	45.9010	-59.3453	5.4334	0.0500	5.3834
3204	49.5664	-62.6437	6.1589	0.0900	6.0689
3205	50.9383	-64.5991	6.5751	0.0900	6.4851
3206	53.8615	-68.0756	7.3154	0.0900	7.2254
3207	57.0759	-73.2634	8.3316	0.0700	8.2616
3208	60.2704	-79.4508	9.6547	0.0500	9.6047
3301	39.1772	-33.3355	2.5073	0.0500	2.4573
3302	49.2493	-37.6024	3.7306	0.0500	3.6806
3303	57.1410	-42.7391	4.8838	0.0500	4.8338
3304	62.9973	-47.8048	6.0009	0.0500	5.9509
3305	65.2145	-50.4852	6.5532	0.0500	6.5032
3306	69.8127	-55.9919	7.7262	0.0500	7.6762
3307	74.9142	-64.2213	9.3794	0.0500	9.3294
3308	79.4083	-74.1105	11.4409	0.0500	11.3909
3401	43.0282	-16.8491	2.0506	0.0500	2.0006
3402	57.5570	-19.4475	3.5145	0.0500	3.4645
3403	68.2880	-26.2355	5.0907	0.0500	5.0407
3404	76.3242	-32.9350	6.6242	0.0500	6.5742
3405	79.3130	-36.4131	7.3646	0.0900	7.2746
3406	85.9804	-44.3854	9.0376	0.0500	8.9876
3407	92.4287	-54.9164	11.1320	0.0700	11.0620
3408	95.6621	-69.6339	13.4965	0.0500	13.4465
3501	61.9067	-9.8741	3.7726	0.0500	3.7226
3502	77.1688	-13.1981	5.8126	0.0500	5.7626
3503	89.6283	-18.1605	7.9575	0.0500	7.9075
3504	93.6654	-22.6604	8.9019	0.0500	8.8519

3505	98.6985	-35.1352	10.5799	0.0500	10.5299
3506	101.9068	-50.4489	12.4686	0.0500	12.4186
3601	97.4221	-8.9365	9.1684	0.0700	9.0984
3602	102.3506	-14.3142	10.2946	0.0700	10.2246
4101	179.9516	-83.3150	38.1654	0.0500	38.1154
4102	180.9599	-80.0690	38.0323	0.0500	37.9823
4103	183.1373	-77.3167	38.3744	0.0900	38.2844
4104	184.2894	-75.1733	38.4897	0.0900	38.3997
4105	185.4376	-73.7870	38.6913	0.0900	38.6013
4106	187.3985	-73.0381	39.1944	0.0500	39.1444
4107	189.8021	-71.5387	39.9656	0.0500	39.9156
4108	193.7239	-70.2583	41.1898	0.0500	41.1398
4201	161.8294	-78.2566	31.4118	0.0700	31.3418
4202	164.2810	-71.5465	31.1476	0.0500	31.0976
4203	167.9926	-66.1407	31.6571	0.0900	31.5671
4204	170.7847	-61.9697	32.0405	0.0900	31.9505
4205	172.4839	-59.9096	32.3777	0.0900	32.2877
4206	176.3381	-57.4522	33.3586	0.0500	33.3086
4207	181.4122	-54.1551	34.7705	0.0500	34.7205
4208	188.5808	-51.3945	37.0578	0.0500	37.0078
4301	143.4660	-73.3582	25.3108	0.0700	25.2408
4302	147.2944	-62.9183	24.9066	0.0500	24.8566
4303	152.6240	-54.9239	25.5570	0.0500	25.5070
4304	156.9365	-48.6140	26.2177	0.0900	26.1277
4305	159.4156	-45.9239	26.7460	0.0900	26.6560
4306	165.1239	-41.6364	28.1636	0.0700	28.0936
4307	173.1775	-36.4103	30.3935	0.0500	30.3435
4308	183.3873	-32.4518	33.6058	0.0500	33.5558
4401	127.6768	-69.2653	20.5239	0.0500	20.4739
4402	130.1991	-54.3337	19.3374	0.0500	19.2874
4403	137.0768	-43.6257	20.1153	0.0500	20.0653
4404	143.0862	-35.2482	21.0627	0.0500	21.0127
4405	146.2644	-31.7037	21.7442	0.0500	21.6942
4406	154.1788	-25.6334	23.7589	0.0500	23.7089
4407	164.6713	-18.7881	26.6236	0.0500	26.5736
4408	178.8449	-16.2704	31.2232	0.0900	31.1332
4501	120.9334	-50.0974	16.6187	0.0500	16.5687
4502	124.4628	-34.9704	16.2182	0.0500	16.1682
4503	128.7368	-22.1634	16.5376	0.0500	16.4876
4504	132.9299	-17.5556	17.4815	0.0500	17.4315
4505	145.1764	-13.0735	20.7308	0.0900	20.6408
4506	160.0735	-9.4261	24.9848	0.0700	24.9148
4601	120.0467	-14.0318	14.1867	0.0900	14.0967
4602	124.5202	-9.0064	15.2426	0.0900	15.1526

Coordinates of Target Points for Set 2 of Metric Camera Measurements

Coordinates shown in inches

Target #	X	Y	Z	Button Thk.	Z corrected
101	174.5905	-0.0769	29.5670	0.0700	29.4970
102	155.6454	-0.0154	23.6356	0.0500	23.5856
103	136.3710	-0.2296	18.1274	0.0700	18.0574
104	116.9656	-0.4123	13.4805	0.0700	13.4105
105	105.3810	-0.2565	10.8334	0.0700	10.7634
106	85.7340	0.1270	7.1549	0.0700	7.0849
107	65.7249	-0.2673	4.2342	0.0700	4.1642
108	46.1811	-0.2733	2.1509	0.0700	2.0809
201	111.7699	65.1274	16.3186	0.0500	16.2686
202	111.4209	45.3467	14.0177	0.0500	13.9677
203	111.5714	25.4650	12.7677	0.0700	12.6977
204	111.1281	5.6126	12.1792	0.0700	12.1092
205	111.0484	-6.1943	12.1138	0.0700	12.0438
206	111.3678	-26.1356	12.6563	0.0500	12.6063
207	111.4710	-46.1084	14.0239	0.0500	13.9739
208	111.7706	-65.6460	16.2816	0.0500	16.2316
301	97.4180	-8.9405	9.1930	0.0900	9.1030
302	98.6600	-10.0961	9.4273	0.0000	9.4273
303	99.8626	-11.4873	9.7226	0.0000	9.7226
304	101.1693	-12.8612	10.0078	0.0000	10.0078
305	102.3526	-14.3144	10.2951	0.0900	10.2051
306	100.9828	-15.6708	10.0543	0.0000	10.0543
307	99.5703	-17.0293	9.8298	0.0000	9.8298
308	98.1289	-18.3625	9.5973	0.0000	9.5973
309	96.7107	-19.8127	9.3663	0.0000	9.3663
310	95.2404	-21.2358	9.1196	0.0000	9.1196
311	93.6840	-22.6781	8.8938	0.0500	8.8438
312	94.1407	-20.6299	8.8903	0.0000	8.8903
313	94.7378	-18.7101	8.9564	0.0000	8.9564
314	95.2382	-16.8272	8.9898	0.0000	8.9898
315	95.7243	-14.7674	9.0222	0.0000	9.0222
316	96.2401	-12.9376	9.0633	0.0000	9.0633
317	96.7964	-10.8840	9.1005	0.0000	9.1005
401	69.7897	-55.9583	7.7065	0.0500	7.6565
402	70.7971	-57.5736	8.0267	0.0000	8.0267
403	71.8464	-59.2107	8.3772	0.0000	8.3772
404	72.8471	-60.8239	8.7037	0.0000	8.7037
405	73.8917	-62.4686	9.0278	0.0000	9.0278
406	74.8949	-64.1706	9.3656	0.0500	9.3156
407	73.2654	-65.0892	9.2521	0.0000	9.2521
408	71.4736	-66.0238	9.1568	0.0000	9.1568
409	69.6523	-66.9082	9.0482	0.0000	9.0482
410	67.8976	-67.8299	8.9523	0.0000	8.9523
411	65.9740	-68.7370	8.8214	0.0000	8.8214
412	64.2344	-69.6505	8.7274	0.0000	8.7274
413	62.4787	-70.5147	8.6125	0.0000	8.6125
414	60.6225	-71.4832	8.5059	0.0000	8.5059
415	58.8392	-72.4000	8.3918	0.0000	8.3918
416	57.0578	-73.2251	8.3183	0.0700	8.2483
417	58.1542	-71.4413	8.1828	0.0000	8.1828
418	59.3113	-69.8436	8.1209	0.0000	8.1209
419	60.3907	-68.1468	8.0383	0.0000	8.0383
420	61.6366	-66.5198	7.9823	0.0000	7.9823
421	62.7227	-65.0813	7.9366	0.0000	7.9366
422	64.0268	-63.3592	7.8815	0.0000	7.8815

423	65.2526	-61.8014	7.8264	0.0000	7.8264
424	66.3943	-60.2853	7.7848	0.0000	7.7848
425	67.4810	-58.6850	7.7230	0.0000	7.7230
426	68.7435	-57.0824	7.6746	0.0000	7.6746
1101	193.4653	70.1757	41.0976	0.0500	41.0476
1102	190.0260	71.5126	40.0350	0.0500	39.9850
1103	187.1052	72.8683	39.1378	0.0500	39.0878
1104	185.2696	74.2336	38.6668	0.0500	38.6168
1105	184.0860	74.9417	38.3437	0.0900	38.2537
1106	182.4023	77.3120	38.1166	0.0900	38.0266
1107	180.7386	79.7811	37.8740	0.0500	37.8240
1108	179.8454	83.3006	38.1333	0.0500	38.0833
1201	188.4898	51.2056	37.0693	0.0500	37.0193
1202	181.9133	53.9608	34.9697	0.0500	34.9197
1203	176.4561	56.9261	33.3808	0.0900	33.2908
1204	172.4925	60.2564	32.3973	0.0500	32.3473
1205	170.5287	61.7247	31.9152	0.0900	31.8252
1206	167.2013	66.2382	31.3985	0.0900	31.3085
1207	164.0644	71.1457	31.0670	0.0900	30.9770
1208	161.7064	78.3821	31.3667	0.0500	31.3167
1301	183.2578	32.2784	33.6760	0.0900	33.5860
1302	173.4777	36.3037	30.5460	0.0900	30.4560
1303	165.1793	41.1158	28.1622	0.0900	28.0722
1304	159.4552	46.1354	26.8011	0.0900	26.7111
1305	156.6821	48.4835	26.1549	0.0900	26.0649
1306	152.0287	54.5992	25.3048	0.0500	25.2548
1307	147.0581	62.5952	24.8185	0.0500	24.7685
1308	143.3695	73.3315	25.2115	0.0500	25.1615
1401	178.7374	16.1214	31.2926	0.0500	31.2426
1402	164.9034	18.7317	26.7524	0.0500	26.7024
1403	154.0119	25.2981	23.6667	0.0500	23.6167
1404	146.3207	31.9156	21.7877	0.0500	21.7377
1405	142.8402	35.0131	21.0247	0.0900	20.9347
1406	136.6147	43.1897	19.9506	0.0500	19.9006
1407	130.0189	53.7970	19.3315	0.0900	19.2415
1408	127.6663	69.0721	20.4787	0.0500	20.4287
1501	160.2863	9.3360	25.0944	0.0500	25.0444
1502	145.0654	12.6251	20.6137	0.0500	20.5637
1503	133.0927	17.6137	17.5568	0.0500	17.5068
1504	128.8196	21.5536	16.5904	0.0500	16.5404
1505	124.2107	34.1629	16.1037	0.0500	16.0537
1506	120.8389	49.4294	16.5669	0.0500	16.5169
1601	124.9248	8.9154	15.3178	0.0900	15.2278
1602	120.1213	13.4476	14.2634	0.0500	14.2134
2101	41.0725	84.3952	8.5777	0.0500	8.5277
2102	39.2546	81.7558	8.0447	0.0900	7.9547
2103	37.7159	79.7052	7.5798	0.0900	7.4898
2104	36.3503	77.7097	7.1764	0.0500	7.1264
2105	35.7947	76.9629	6.9941	0.0500	6.9441
2106	34.2228	75.6442	6.7311	0.0500	6.6811
2107	32.0916	73.3648	6.2841	0.0500	6.2341
2108	29.8281	71.4735	5.8497	0.0500	5.7997
2201	60.3728	79.2114	9.6982	0.0500	9.6482
2202	57.2443	73.0945	8.3911	0.0500	8.3411
2203	53.9368	68.0377	7.4615	0.0900	7.3715
2204	50.9952	64.1278	6.5675	0.0500	6.5175
2205	49.3981	62.3388	6.1637	0.0500	6.1137
2206	45.6152	59.2814	5.4426	0.0500	5.3926
2207	40.7186	55.4282	4.5972	0.0900	4.5072
2208	34.8773	52.2122	3.9047	0.0500	3.8547

2301	79.4348	73.6494	11.4090	0.0500	11.3590
2302	75.0006	63.7987	9.4104	0.0900	9.3204
2303	70.0192	56.0909	7.8001	0.0500	7.7501
2304	65.3291	50.0802	6.5674	0.0500	6.5174
2305	62.9541	47.6350	6.0698	0.0500	6.0198
2306	57.1604	42.8419	4.9206	0.0500	4.8706
2307	49.3927	37.3093	3.7497	0.0500	3.6997
2308	39.5509	32.8765	2.5346	0.0500	2.4846
2401	95.6787	69.0981	13.4975	0.0500	13.4475
2402	92.5796	54.5920	11.1965	0.0900	11.1065
2403	85.8231	44.0220	9.0701	0.0500	9.0201
2404	79.3932	35.9454	7.4257	0.0900	7.3357
2405	76.2607	32.7085	6.6780	0.0500	6.6280
2406	68.3977	26.4295	5.2618	0.0500	5.2118
2407	57.6962	19.2298	3.6141	0.0500	3.5641
2408	43.1829	16.3003	2.1092	0.0500	2.0592
2501	101.9550	49.8683	12.4352	0.0500	12.3852
2502	98.3568	34.4961	10.6452	0.0900	10.5552
2503	93.7079	22.1465	9.0050	0.0500	8.9550
2504	89.6197	17.9887	8.1458	0.0500	8.0958
2505	77.1924	13.3024	5.9520	0.0500	5.9020
2506	62.0014	9.5889	3.8173	0.0500	3.7673
2601	102.3090	13.7524	10.3679	0.0500	10.3179
2602	97.6368	8.9350	9.3835	0.0900	9.2935
3101	30.1254	-72.0812	5.8798	0.0500	5.8298
3102	32.2619	-73.7325	6.3120	0.0500	6.2620
3103	34.4270	-75.6890	6.7310	0.0500	6.6810
3104	36.0395	-77.3816	7.1005	0.0900	7.0105
3105	36.5212	-78.4165	7.3104	0.0900	7.2204
3106	37.8119	-80.0416	7.6477	0.0900	7.5577
3107	39.2022	-82.2463	8.0917	0.0700	8.0217
3108	41.0392	-84.7999	8.6867	0.0500	8.6367
3201	34.6113	-52.7300	3.8580	0.0500	3.8080
3202	40.8788	-55.7801	4.6165	0.0500	4.5665
3203	45.9069	-59.3677	5.4270	0.0500	5.3770
3204	49.5567	-62.6512	6.1494	0.0900	6.0594
3205	50.9298	-64.6058	6.5634	0.0900	6.4734
3206	53.8425	-68.0572	7.3011	0.0900	7.2111
3207	57.0582	-73.2252	8.3181	0.0700	8.2481
3208	60.2682	-79.4140	9.6417	0.0500	9.5917
3301	39.1803	-33.3608	2.5202	0.0500	2.4702
3302	49.2277	-37.6097	3.7429	0.0500	3.6929
3303	57.1426	-42.7528	4.8760	0.0500	4.8260
3304	63.0228	-47.8360	5.9911	0.0500	5.9411
3305	65.2197	-50.4978	6.5392	0.0500	6.4892
3306	69.7898	-55.9586	7.7059	0.0500	7.6559
3307	74.8950	-64.1709	9.3652	0.0500	9.3152
3308	79.4122	-74.0757	11.4254	0.0500	11.3754
3401	43.0451	-16.8738	2.0715	0.0500	2.0215
3402	57.5391	-19.4638	3.5647	0.0500	3.5147
3403	68.2398	-26.2196	5.1136	0.0500	5.0636
3404	76.3289	-32.9431	6.6143	0.0500	6.5643
3405	79.3239	-36.4265	7.3553	0.0900	7.2653
3406	85.9866	-44.3876	9.0259	0.0500	8.9759
3407	92.4230	-54.8847	11.1173	0.0700	11.0473
3408	95.6652	-69.5822	13.4764	0.0500	13.4264
3501	61.9137	-9.8994	3.8290	0.0500	3.7790
3502	77.1822	-13.2235	5.8499	0.0500	5.7999
3503	89.6547	-18.1897	7.9655	0.0500	7.9155
3504	93.6840	-22.6783	8.8931	0.0500	8.8431

3505	98.6790	-35.1000	10.5672	0.0500	10.5172
3506	101.9170	-50.4477	12.4609	0.0500	12.4109
3601	97.4179	-8.9403	9.1926	0.0700	9.1226
3602	102.3524	-14.3142	10.2949	0.0700	10.2249
4101	179.9744	-83.3223	38.1623	0.0500	38.1123
4102	180.9966	-80.0542	38.0306	0.0500	37.9806
4103	183.1690	-77.3134	38.3750	0.0900	38.2850
4104	184.3149	-75.1802	38.4904	0.0900	38.4004
4105	185.4727	-73.7831	38.6923	0.0900	38.6023
4106	187.4140	-73.0492	39.1967	0.0500	39.1467
4107	189.8274	-71.5449	39.9692	0.0500	39.9192
4108	193.7420	-70.2662	41.1936	0.0500	41.1436
4201	161.8564	-78.2548	31.4048	0.0700	31.3348
4202	164.3060	-71.5498	31.1413	0.0500	31.0913
4203	168.0167	-66.1453	31.6537	0.0900	31.5637
4204	170.8057	-61.9768	32.0393	0.0900	31.9493
4205	172.4936	-59.9265	32.3754	0.0900	32.2854
4206	176.3292	-57.4784	33.3561	0.0500	33.3061
4207	181.3843	-54.1826	34.7691	0.0500	34.7191
4208	188.5732	-51.4042	37.0626	0.0500	37.0126
4301	143.4915	-73.3405	25.3030	0.0700	25.2330
4302	147.3189	-62.9170	24.8911	0.0500	24.8411
4303	152.6421	-54.9293	25.5504	0.0500	25.5004
4304	156.9345	-48.6380	26.2163	0.0900	26.1263
4305	159.3923	-45.9646	26.7427	0.0900	26.6527
4306	165.1268	-41.6500	28.1721	0.0700	28.1021
4307	173.1720	-36.4212	30.3946	0.0500	30.3446
4308	183.3958	-32.4526	33.6108	0.0500	33.5608
4401	127.6992	-69.2565	20.5039	0.0500	20.4539
4402	130.2255	-54.3187	19.3241	0.0500	19.2741
4403	137.1010	-43.6190	20.1044	0.0500	20.0544
4404	143.1086	-35.2424	21.0589	0.0500	21.0089
4405	146.2682	-31.7149	21.7419	0.0500	21.6919
4406	154.1876	-25.6359	23.7736	0.0500	23.7236
4407	164.6711	-18.7922	26.6234	0.0500	26.5734
4408	178.8018	-16.2816	31.2263	0.0900	31.1363
4501	120.9585	-50.0807	16.6059	0.0500	16.5559
4502	124.4700	-34.9822	16.2117	0.0500	16.1617
4503	128.7316	-22.1823	16.5365	0.0500	16.4865
4504	132.9274	-17.5688	17.4774	0.0500	17.4274
4505	145.1646	-13.0890	20.7525	0.0900	20.6625
4506	160.0727	-9.4278	24.9878	0.0700	24.9178
4601	120.0613	-14.0268	14.1897	0.0900	14.0997
4602	124.4985	-9.0363	15.2415	0.0900	15.1515

APPENDIX C

Program listing for Solving Set 1 'Best-Fit' Surface

```
10 DIM XIII(200),YIII(200),ZII(200),NOD(200),ZP(200),X(200),Y(200),Z(200)
20 DIM XI(200),XII(200),YII(200),YI(200),ZI(200),ZIII(200)
30 OPEN "B:XYZTRN1" FOR INPUT AS #1
40 FOCAL=258!:DELTAZ=0!:DELTAX=0:DELTAY=0!:RMSMINT=1:RMSMINP=1
50 N=0
60 INPUT #1,NODE,D1,D2,D3,D4
70 IF NODE>300 AND NODE<599 THEN GOTO 60
80 N=N+1:NOD(N)=NODE:XIII(N)=D1:YIII(N)=D2:ZIII(N)=D3-(D4*.02+.01)
90 IF NODE=4602 THEN NNODE=N:GOTO 100 ELSE GOTO 60
100 BETA=0!:ALPHA=0
110 DELTAZ=0:DELTAY=0:DELTAX=0
120 FOR I=1 TO NNODE:XII(I)=XIII(I)+DELTAX:YII(I)=YIII(I)+DELTAY:ZII(I)=ZIII(I)+
DELTAZ:NEXT I
130 ALPHARAD=ALPHA*3.1415927#/180!
140 FOR I=1 TO NNODE:YI(I)=YII(I)*COS(ALPHARAD)+ZII(I)*SIN(ALPHARAD)
150 ZI(I)=-YII(I)*SIN(ALPHARAD)+ZII(I)*COS(ALPHARAD)
160 XI(I)=XII(I)
170 NEXT I
180 BETARAD=BETA*3.1415927#/180!
190 FOR I=1 TO NNODE:X(I)=XI(I)*COS(BETARAD)+ZI(I)*SIN(BETARAD)
200 Z(I)=-XI(I)*SIN(BETARAD)+ZI(I)*COS(BETARAD)
210 Y(I)=YI(I):NEXT I
220 FOR I=1 TO NNODE:ZP(I)=(X(I)*X(I)+Y(I)*Y(I))/(4!*FOCAL):NEXT I
230 REM PRINT " NODE          X          Y          Z          ZP          DELTAZ"
240 REM FOR I=1 TO NNODE:IF ABS(Z(I)-ZP(I))<.1 THEN GOTO 270
250 REM PRINT USING "####   ";NOD(I);
260 REM PRINT USING "####.####   ";X(I);Y(I);Z(I);ZP(I);Z(I)-ZP(I)
270 REM NEXT I
280 NNODA=0:NNODB=0:NNODC=0:NNODD=0
290 RMSA=0:RMSB=0:RMSC=0:RMSD=0:AVEA=0:AVEB=0:AVEC=0:AVED=0
300 FOR I=1 TO NNODE:IF NOD(I)>1000 AND NOD(I)<2000 THEN NNODA=NNODA+1:RMSA=RMSA
+(Z(I)-ZP(I))*(Z(I)-ZP(I)):AVEA=AVEA+(Z(I)-ZP(I))
310 IF NOD(I)>2000 AND NOD(I)<3000 THEN NNODB=NNODB+1:RMSB=RMSB+(Z(I)-ZP(I))*(Z(
I)-ZP(I)):AVEB=AVEB+(Z(I)-ZP(I))
320 IF NOD(I)>3000 AND NOD(I)<4000 THEN NNODC=NNODC+1:RMSC=RMSC+(Z(I)-ZP(I))*(Z(
I)-ZP(I)):AVEC=AVEC+(Z(I)-ZP(I))
330 IF NOD(I)>4000 AND NOD(I)<5000 THEN NNODD=NNODD+1:RMSD=RMSD+(Z(I)-ZP(I))*(Z(
I)-ZP(I)):AVED=AVED+(Z(I)-ZP(I))
340 NEXT I
350 PRINT "DELTAX =";DELTAX;" DELTAY =";DELTAY;" DELTAZ =";DELTAZ
360 PRINT "ALPHA =";ALPHA;"  BETA =";BETA
370 PRINT "FOCAL LENGTH =";FOCAL
380 PRINT "AVE ERROR IN QUAD A =";AVEA/NNODA;" RMS ERROR IN QUAD A =";SQR(RMSA/N
NODA)
390 PRINT "AVE ERROR IN QUAD B =";AVEB/NNODB;" RMS ERROR IN QUAD B =";SQR(RMSB/N
NODB)
400 PRINT "AVE ERROR IN QUAD C =";AVEC/NNODC;" RMS ERROR IN QUAD C =";SQR(RMSC/N
NODC)
410 PRINT "AVE ERROR IN QUAD D =";AVED/NNODD;" RMS ERROR IN QUAD D =";SQR(RMSD/N
NODD)
420 RMS1=0:N=0:FOR I=1 TO NNODE
430 N=N+1:RMS1=RMS1+((Z(I)-ZP(I))*(Z(I)-ZP(I)))
440 NEXT I
450 RMSTOT=SQR(RMS1/N)
460 RMS2=0:N=0:FOR I=1 TO NNODE
470 IF NOD(I)>3000 AND NOD(I)<4000 THEN GOTO 490
480 N=N+1:RMS2=RMS2+((Z(I)-ZP(I))*(Z(I)-ZP(I)))
```

ORIGINAL PAGE IS
OF POOR QUALITY

ORIGINAL PAGE IS
OF POOR QUALITY

```
490 NEXT I
500 RMSPAR=SQR(RMS2/N)
501 GOSUB 10000
510 PRINT "RMS SURFACE ERROR =";RMSTOT
520 PRINT "RMS WITHOUT QUAD C =";RMSPAR
521 PRINT "***********  MIN RMS INFO  ***********"
522 PRINT "WHOLE SURFACE:":PRINT "FOCAL =";FOCALT
523 PRINT "DELTAX =";DXT;"DELTAY =";DYT;"DELTAZ =";DZT
524 PRINT "ALPHA =";ALPHAT;"BETA =";BETAT
525 PRINT "RMS =";RMSMINT
526 PRINT "PARTIAL SURFACE:":PRINT "FOCAL =";FOCALP
527 PRINT "DELTAX =";DXP;"DELTAY =";DYP;"DELTAZ =";DZP
528 PRINT "ALPHA =";ALPHAP;"BETA =";BETAP
529 PRINT "RMS =";RMSMINP
530 PRINT "DO YOU WANT HARDCOPY OF THE INFORMATION (Y/N)":INPUT A$
540 IF A$<>"Y" THEN GOTO 740
550 LPRINT "FOCAL LENGTH =";FOCAL
560 LPRINT "DELTAX =";DELTAX
570 LPRINT "DELTAY =";DELTAY
580 LPRINT "DELTAZ =";DELTAZ
590 LPRINT "ALPHA =";ALPHA
600 LPRINT "BETA =";BETA
610 LPRINT "AVE ERROR IN QUAD A =";AVEA/NNODA;" RMS ERROR IN QUAD A =";SQR(RMSA/
NNODA)
620 LPRINT "AVE ERROR IN QUAD B =";AVEB/NNODB;" RMS ERROR IN QUAD B =";SQR(RMSB/
NNODB)
630 LPRINT "AVE ERROR IN QUAD C =";AVEC/NNODC;" RMS ERROR IN QUAD C =";SQR(RMSC/
NNODC)
640 LPRINT "AVE ERROR IN QUAD D =";AVED/NNODD;" RMS ERROR IN QUAD D =";SQR(RMSD/
NNODD)
650 LPRINT "RMS TOTAL SURFACE ERROR =";RMSTOT
660 LPRINT "RMS SURFACE ERROR WITHOUT QUAD C =";RMSPAR
670 LPRINT "*************************************************************************
"
680 LPRINT " NODE      X          Y          Z          ZP        DELTAZ      DELTAZ^2
"
690 FOR I=1 TO NNODE:LPRINT USING "####  ";NOD(I);
700 LPRINT USING "####.#### ";X(I);Y(I);Z(I);ZP(I);Z(I)-ZP(I);(Z(I)-ZP(I))^2;
710 IF ABS(Z(I)-ZP(I))>.1 THEN LPRINT "****" ELSE LPRINT " "
720 NEXT I
730 LPRINT CHR$(12)
740 PRINT "DO YOU WANT TO CHANGE SOME PARAMETERS (Y/N)":INPUT A$
750 IF A$<>"Y" THEN END
760 INPUT "ENTER NEW VALUE FOR DELTAX ",DELTAXNEW
770 INPUT "ENTER NEW VALUE FOR DELTAY ",DELTAYNEW
780 INPUT "ENTER NEW VALUE FOR DELTAZ ",DELTAZNEW
790 INPUT "ENTER NEW VALUE FOR ALPHA IN DEG. ",ALPHANEW
800 INPUT "ENTER NEW VALUE FOR BETA IN DEG.",BETANEW
810 INPUT "ENTER NEW FOCAL LENGTH ",FOCALNEW
820 IF DELTAXNEW<>DELTAX OR DELTAYNEW<>DELTAY OR DELTAZNEW<>DELTAZ THEN DELTAX=D
ELTAXNEW:DELTAY=DELTAYNEW:DELTAZ=DELTAZNEW:ALPHA=ALPHANEW:BETA=BETANEW:FOCAL=FOC
ALNEW:GOTO 120
830 IF ALPHANEW<>ALPHA THEN FOCAL=FOCALNEW:BETA=BETANEW:ALPHA=ALPHANEW:GOTO 130
840 IF BETANEW<>BETA THEN FOCAL=FOCALNEW:BETA=BETANEW:GOTO 180
850 FOCAL=FOCALNEW:GOTO 220
10000 IF RMSTOT<RMSMINT THEN RMSMINT=RMSTOT:DXT=DELTAX:DYT=DELTAY:DZT=DELTAZ:ALP
HAT=ALPHA:BETAT=BETA:FOCALT=FOCAL
10010 IF RMSPAR<RMSMINP THEN RMSMINP=RMSPAR:DXP=DELTAX:DYP=DELTAY:DZP=DELTAZ:ALP
HAP=ALPHA:BETAP=BETA:FOCALP=FOCAL
10020 RETURN
```

Program listing for Solving Set 2 'Best-Fit' Surface

```
10 DIM XIII(200),YIII(200),ZII(200),NOD(200),ZP(200),X(200),Y(200),Z(200)
20 DIM XI(200),XII(200),YII(200),YI(200),ZI(200),ZIII(200)
30 OPEN "B:XYZTRN2" FOR INPUT AS #1
35 OPEN "B:BUTTON.DAT" FOR INPUT AS #2
40 FOCAL=258!:DELTAZ=0!:DELTAX=0:DELTAY=0!:RMSMINT=1:RMSMINP=1
50 N=0
60 INPUT #1,NODE,D1,D2,D3:INPUT #2,DUM,D4
70 IF NODE>300 AND NODE<599 THEN GOTO 60
80 N=N+1:NOD(N)=NODE:XIII(N)=D1:YIII(N)=D2:ZIII(N)=D3-(D4*.02+.01)
90 IF NODE=4602 THEN NNODE=N:GOTO 100 ELSE GOTO 60
100 BETA=0!:ALPHA=0
110 DELTAZ=0:DELTAY=0:DELTAX=0
120 FOR I=1 TO NNODE:XII(I)=XIII(I)+DELTAX:YII(I)=YIII(I)+DELTAY:ZII(I)=ZIII(I)+
DELTAZ:NEXT I
130 ALPHARAD=ALPHA*3.1415927#/180!
140 FOR I=1 TO NNODE:YI(I)=YII(I)*COS(ALPHARAD)+ZII(I)*SIN(ALPHARAD)
150 ZI(I)=-YII(I)*SIN(ALPHARAD)+ZII(I)*COS(ALPHARAD)
160 XI(I)=XII(I)
170 NEXT I
180 BETARAD=BETA*3.1415927#/180!
190 FOR I=1 TO NNODE:X(I)=XI(I)*COS(BETARAD)+ZI(I)*SIN(BETARAD)
200 Z(I)=-XI(I)*SIN(BETARAD)+ZI(I)*COS(BETARAD)
210 Y(I)=YI(I):NEXT I
220 FOR I=1 TO NNODE:ZP(I)=(X(I)*X(I)+Y(I)*Y(I))/(4!*FOCAL):NEXT I
230 REM PRINT " NODE          X          Y          Z          ZP          DELTAZ"
240 REM FOR I=1 TO NNODE:IF ABS(Z(I)-ZP(I))<.1 THEN GOTO 270
250 REM PRINT USING "####  ";NOD(I);
260 REM PRINT USING "####.####  ";X(I);Y(I);Z(I);ZP(I);Z(I)-ZP(I)
270 REM NEXT I
280 NNODA=0:NNODB=0:NNODC=0:NNODD=0
290 RMSA=0:RMSB=0:RMSC=0:RMSD=0:AVEA=0:AVEB=0:AVEC=0:AVED=0
300 FOR I=1 TO NNODE:IF NOD(I)>1000 AND NOD(I)<2000 THEN NNODA=NNODA+1:RMSA=RMSA
+(Z(I)-ZP(I))*(Z(I)-ZP(I)):AVEA=AVEA+(Z(I)-ZP(I))
310 IF NOD(I)>2000 AND NOD(I)<3000 THEN NNODB=NNODB+1:RMSB=RMSB+(Z(I)-ZP(I))*(Z(
I)-ZP(I)):AVEB=AVEB+(Z(I)-ZP(I))
320 IF NOD(I)>3000 AND NOD(I)<4000 THEN NNODC=NNODC+1:RMSC=RMSC+(Z(I)-ZP(I))*(Z(
I)-ZP(I)):AVEC=AVEC+(Z(I)-ZP(I))
330 IF NOD(I)>4000 AND NOD(I)<5000 THEN NNODD=NNODD+1:RMSD=RMSD+(Z(I)-ZP(I))*(Z(
I)-ZP(I)):AVED=AVED+(Z(I)-ZP(I))
340 NEXT I
350 PRINT "DELTAX =";DELTAX;" DELTAY =";DELTAY;" DELTAZ =";DELTAZ
360 PRINT "ALPHA =";ALPHA;"  BETA =";BETA
370 PRINT "FOCAL LENGTH =";FOCAL
380 PRINT "AVE ERROR IN QUAD A =";AVEA/NNODA;" RMS ERROR IN QUAD A =";SQR(RMSA/N
NODA)
390 PRINT "AVE ERROR IN QUAD B =";AVEB/NNODB;" RMS ERROR IN QUAD B =";SQR(RMSB/N
NODB)
400 PRINT "AVE ERROR IN QUAD C =";AVEC/NNODC;" RMS ERROR IN QUAD C =";SQR(RMSC/N
NODC)
410 PRINT "AVE ERROR IN QUAD D =";AVED/NNODD;" RMS ERROR IN QUAD D =";SQR(RMSD/N
NODD)
420 RMS1=0:N=0:FOR I=1 TO NNODE
430 N=N+1:RMS1=RMS1+((Z(I)-ZP(I))*(Z(I)-ZP(I)))
440 NEXT I
450 RMSTOT=SQR(RMS1/N)
460 RMS2=0:N=0:FOR I=1 TO NNODE
470 IF NOD(I)>3000 AND NOD(I)<4000 THEN GOTO 490
480 N=N+1:RMS2=RMS2+((Z(I)-ZP(I))*(Z(I)-ZP(I)))
```

```
490 NEXT I
500 RMSPAR=SQR(RMS2/N)
501 GOSUB 10000
510 PRINT "RMS SURFACE ERROR =";RMSTOT
520 PRINT "RMS WITHOUT QUAD C =";RMSPAR
521 PRINT "***********  MIN RMS INFO  ***********"
522 PRINT "WHOLE SURFACE:":PRINT "FOCAL =";FOCALT
523 PRINT "DELTAX =";DXT;"DELTAY =";DYT;"DELTAZ =";DZT
524 PRINT "ALPHA =";ALPHAT;"BETA =";BETAT
525 PRINT "RMS =";RMSMINT
526 PRINT "PARTIAL SURFACE:":PRINT "FOCAL =";FOCALP
527 PRINT "DELTAX =";DXP;"DELTAY =";DYP;"DELTAZ =";DZP
528 PRINT "ALPHA =";ALPHAP;"BETA =";BETAP
529 PRINT "RMS =";RMSMINP
530 PRINT "DO YOU WANT HARDCOPY OF THE INFORMATION (Y/N)":INPUT A$
540 IF A$<>"Y" THEN GOTO 740
550 LPRINT "FOCAL LENGTH =";FOCAL
560 LPRINT "DELTAX =";DELTAX
570 LPRINT "DELTAY =";DELTAY
580 LPRINT "DELTAZ =";DELTAZ
590 LPRINT "ALPHA =";ALPHA
600 LPRINT "BETA =";BETA
610 LPRINT "AVE ERROR IN QUAD A =";AVEA/NNODA;" RMS ERROR IN QUAD A =";SQR(RMSA/
NNODA)
620 LPRINT "AVE ERROR IN QUAD B =";AVEB/NNODB;" RMS ERROR IN QUAD B =";SQR(RMSB/
NNODB)
630 LPRINT "AVE ERROR IN QUAD C =";AVEC/NNODC;" RMS ERROR IN QUAD C =";SQR(RMSC/
NNODC)
640 LPRINT "AVE ERROR IN QUAD D =";AVED/NNODD;" RMS ERROR IN QUAD D =";SQR(RMSD/
NNODD)
650 LPRINT "RMS TOTAL SURFACE ERROR =";RMSTOT
660 LPRINT "RMS SURFACE ERROR WITHOUT QUAD C =";RMSPAR
670 LPRINT "*************************************************************************
"
680 LPRINT " NODE      X          Y          Z          ZP        DELTAZ      DELTAZ^2
"
690 FOR I=1 TO NNODE:LPRINT USING "####  ";NOD(I);
700 LPRINT USING "####.#### ";X(I);Y(I);Z(I);ZP(I);Z(I)-ZP(I);(Z(I)-ZP(I))^2;
710 IF ABS(Z(I)-ZP(I))>.1 THEN LPRINT "****" ELSE LPRINT " "
720 NEXT I
730 LPRINT CHR$(12)
740 PRINT "DO YOU WANT TO CHANGE SOME PARAMETERS (Y/N)":INPUT A$
750 IF A$<>"Y" THEN END
760 INPUT "ENTER NEW VALUE FOR DELTAX ",DELTAXNEW
770 INPUT "ENTER NEW VALUE FOR DELTAY ",DELTAYNEW
780 INPUT "ENTER NEW VALUE FOR DELTAZ ",DELTAZNEW
790 INPUT "ENTER NEW VALUE FOR ALPHA IN DEG. ",ALPHANEW
800 INPUT "ENTER NEW VALUE FOR BETA IN DEG.",BETANEW
810 INPUT "ENTER NEW FOCAL LENGTH ",FOCALNEW
820 IF DELTAXNEW<>DELTAX OR DELTAYNEW<>DELTAY OR DELTAZNEW<>DELTAZ THEN DELTAX=D
ELTAXNEW:DELTAY=DELTAYNEW:DELTAZ=DELTAZNEW:ALPHA=ALPHANEW:BETA=BETANEW:FOCAL=FOC
ALNEW:GOTO 120
830 IF ALPHANEW<>ALPHA THEN FOCAL=FOCALNEW:BETA=BETANEW:ALPHA=ALPHANEW:GOTO 130
840 IF BETANEW<>BETA THEN FOCAL=FOCALNEW:BETA=BETANEW:GOTO 180
850 FOCAL=FOCALNEW:GOTO 220
10000 IF RMSTOT<RMSMINT THEN RMSMINT=RMSTOT:DXT=DELTAX:DYT=DELTAY:DZT=DELTAZ:ALP
HAT=ALPHA:BETAT=BETA:FOCALT=FOCAL
10010 IF RMSPAR<RMSMINP THEN RMSMINP=RMSPAR:DXP=DELTAX:DYP=DELTAY:DZP=DELTAZ:ALP
HAP=ALPHA:BETAP=BETA:FOCALP=FOCAL
10020 RETURN
```

APPENDIX D

Program listing for Solving Pillow I RMS Error

```
1 REM THIS PROGRAM IS FOR MESH PILLOW I IT ADD ADDITIONAL
2 REM POINTS BY INTERPOLATING BETWEEN EXISTING POINTS
3 REM THIS PROGRAM WORKS IDENTICALLY TO "RMSPIL2.TXT"
4 REM "RMSPIL2.TXT" IS FOR PILLOW II
5 DEFDBL A-H,J-Z
10 DIM ZP(40),ZP2(40),NOD(40),DIST(40),X(40),Y(40),Z(40),Z2(40),DIST2(40)
30 OPEN "B:XYZTRN1" FOR INPUT AS #1
40 FOCAL=258!:DELTAZ=0!:DELTAX=0:DELTAY=0!
45 RMSMIN=100
50 N=0
60 INPUT #1,NODE,D1,D2,D3,D4
70 IF NODE<301 OR NODE>320 THEN GOTO 60
80 N=N+1:NOD(N)=NODE:X(N)=D1:Y(N)=D2:Z(N)=D3-(D4*.02+.01)
90 IF NODE=317 THEN GOTO 100 ELSE GOTO 60
100 N=N+1:NOD(N)=1001:X(N)=(X(9)+X(13))/2!
110 Y(N)=(Y(9)+Y(13))/2!
120 Z(N)=(Z(9)+Z(13))/2!
130 N=N+1:NOD(N)=1002:X(N)=(X(8)+X(14))/2!
140 Y(N)=(Y(8)+Y(14))/2!
150 Z(N)=(Z(8)+Z(14))/2!
160 N=N+1:NOD(N)=1003:X(N)=(X(7)+X(15))/2!
170 Y(N)=(Y(7)+Y(15))/2!
180 Z(N)=(Z(7)+Z(15))/2!
190 N=N+1:NOD(N)=1004:X(N)=(X(16)-X(6))/3+X(6)
200 Y(N)=(Y(16)-Y(6))/3+Y(6)
210 Z(N)=(Z(16)-Z(6))/3+Z(6)
220 N=N+1:NOD(N)=1005:X(N)=(X(16)-X(6))*2/3+X(6)
230 Y(N)=(Y(16)-Y(6))*2/3+Y(6)
240 Z(N)=(Z(16)-Z(6))*2/3+Z(6)
250 N=N+1:NOD(N)=1006:X(N)=(X(16)+X(3))/2!
260 Y(N)=(Y(3)+Y(16))/2!
270 Z(N)=(Z(3)+Z(16))/2!
280 N=N+1:NOD(N)=1007:X(N)=(X(22)+X(4))/2!
290 Y(N)=(Y(4)+Y(22))/2!
300 Z(N)=(Z(4)+Z(22))/2!
310 N=N+1:NOD(N)=1008:X(N)=(X(6)+X(4))/2!
320 Y(N)=(Y(4)+Y(6))/2!
330 Z(N)=(Z(4)+Z(6))/2!
350 NNODE=N
360 FOR I=1 TO NNODE:Z2(I)=(X(I)*X(I)+Y(I)*Y(I))/(4!*258)
370 NEXT I
1000 A=-5.35097:B=1!:C=28.1793:D=274.42352#
1010 A2=-6.0544:B2=1!:C2=32.75341:D2=295.00868#
1020 FOR I=1 TO NNODE:T=(-D-A*X(I)-B*Y(I)-C*Z(I))/(A*A+B*B+C*C)
1030 XP=A*T+X(I):YP=B*T+Y(I):ZP(I)=C*T+Z(I)
1040 DIST(I)=SQR((XP-X(I))*(XP-X(I))+(YP-Y(I))*(YP-Y(I))+(ZP(I)-Z(I))*(ZP(I)-Z(I
)))
1050 NEXT I
1060 FOR I=1 TO NNODE:T2=(-D2-A2*X(I)-B2*Y(I)-C2*Z2(I))/(A2*A2+B2*B2+C2*C2)
1070 XP2=A2*T2+X(I):YP2=B2*T2+Y(I):ZP2(I)=C2*T2+Z2(I)
1080 DIST2(I)=SQR((XP2-X(I))*(XP2-X(I))+(YP2-Y(I))*(YP2-Y(I))+(ZP2(I)-Z2(I))*(ZP
2(I)-Z2(I)))
1090 NEXT I
1100 RMS1=0:FOR I=1 TO NNODE:IF NOD(I)>=301 AND NOD(I)<=317 THEN MULT=1 ELSE MUL
T=2
1104 IF NOD(I)=301 OR NOD(I)=305 THEN MULT=0
1105 RMS1=RMS1+MULT*((DIST(I)+DIST2(I)-DELTAZ)*(DIST(I)+DIST2(I)-DELTAZ))
```

```
1107 PRINT NOD(I);MULT
1110 NEXT I
1120 RMS=SQR(RMS1/(NNODE+6)):IF RMS<RMSMIN THEN RMSMIN=RMS:DELTAZMIN=DELTAZ
1130 REM PRINT " NODE       X          Y          Z          DIST       DIST2      DELTA"
1140 REM FOR I=1 TO NNODE
1150 REM PRINT USING "#### ";NOD(I);
1160 REM PRINT USING "####.#### ";X(I);Y(I);Z(I);DIST(I);DIST2(I);DIST(I)+DIST2(
I)-DELTAZ
1170 REM NEXT I
1180 PRINT "DELTAZ =";DELTAZ;"  RMS ERROR =";RMS
1190 PRINT "MIN DELTAZ =";DELTAZMIN;"MIN RMS ERROR =";RMSMIN
1200 PRINT "DO YOU WANT HARDCOPY OF THE INFORMATION (Y/N)":INPUT A$
1210 IF A$<>"Y" THEN GOTO 1310
1220 WIDTH "LPT1:",130
1230 LPRINT "DELTAZ =";DELTAZ
1240 LPRINT "RMS ERROR =";RMS
1250 LPRINT CHR$(27);"&k2S"
1260 LPRINT " NODE       X          Y          Z          ZP         Z2         ZP2
  DIST       DIST2      DELTA"
1270 FOR I=1 TO NNODE:LPRINT USING "####  ";NOD(I);
1280 LPRINT USING "####.#### ";X(I);Y(I);Z(I);ZP(I);Z2(I);ZP2(I);DIST(I);DIST2(I
);DIST(I)+DIST2(I)-DELTAZ
1290 NEXT I
1300 LPRINT CHR$(12)
1310 INPUT "ENTER NEW VALUE FOR DELTAZ ",DELTAZ
1320 GOTO 1100
```

Program listing for Solving Pillow II RMS Error

```
5 REM THIS PROGRAM IS FOR MESH PILLOW NUMBER II
7 REM IT USES LINEAR INTERPOLATION OF KNOWN POINTS TO ADD TO THE
8 REM POINTS ALREADY KNOWN AND MULTIPLIES THOSES POINTS TWICE
10 DEFDBL A-H,J-Z
20 DIM ZP(40),ZP2(40),NOD(40),DIST(40),X(40),Y(40),Z(40),Z2(40),DIST2(40)
30 OPEN "B:XYZTRN1" FOR INPUT AS #1
40 FOCAL=258!:DELTAZ=0!:DELTAX=0:DELTAY=0!
50 RMSMIN=100
60 N=0
70 INPUT #1,NODE,D1,D2,D3,D4
80 IF NODE<401 OR NODE>430 THEN GOTO 70
90 N=N+1:NOD(N)=NODE:X(N)=D1:Y(N)=D2:Z(N)=D3-(D4*.02+.01)
100 IF NODE=426 THEN GOTO 110 ELSE GOTO 70
110 N=N+1:NOD(N)=1001:X(N)=(X(14)+X(18))/2!
120 Y(N)=(Y(14)+Y(18))/2!
130 Z(N)=(Z(14)+Z(18))/2!
140 N=N+1:NOD(N)=1002:X(N)=(X(13)+X(19))/2!
150 Y(N)=(Y(13)+Y(19))/2!
160 Z(N)=(Z(13)+Z(19))/2!
170 N=N+1:NOD(N)=1003:X(N)=(X(12)+X(20))/2!
180 Y(N)=(Y(12)+Y(20))/2!
190 Z(N)=(Z(12)+Z(20))/2!
200 N=N+1:NOD(N)=1004:X(N)=(X(11)+X(21))/2!
210 Y(N)=(Y(11)+Y(21))/2!
220 Z(N)=(Z(11)+Z(21))/2!
230 N=N+1:NOD(N)=1005:X(N)=(X(10)+X(22))/2!
240 Y(N)=(Y(10)+Y(22))/2!
250 Z(N)=(Z(10)+Z(22))/2!
260 N=N+1:NOD(N)=1006:X(N)=(X(23)-X(9))/3+X(9)
270 Y(N)=(Y(23)-Y(9))/3+Y(9)
280 Z(N)=(Z(23)-Z(9))/3+Z(9)
290 N=N+1:NOD(N)=1007:X(N)=(X(23)-X(9))*2/3+X(9)
300 Y(N)=(Y(23)-Y(9))*2/3+Y(9)
310 Z(N)=(Z(23)-Z(9))*2/3+Z(9)
320 N=N+1:NOD(N)=1008:X(N)=(X(24)-X(8))/3+X(8)
330 Y(N)=(Y(24)-Y(8))/3+Y(8)
340 Z(N)=(Z(24)-Z(8))/3+Z(8)
350 N=N+1:NOD(N)=1009:X(N)=(X(24)-X(8))*2/3+X(8)
360 Y(N)=(Y(24)-Y(8))*2/3+Y(8)
370 Z(N)=(Z(24)-Z(8))*2/3+Z(8)
380 N=N+1:NOD(N)=1010:X(N)=(X(35)+X(5))/2!
390 Y(N)=(Y(5)+Y(35))/2!
400 Z(N)=(Z(5)+Z(35))/2!
410 N=N+1:NOD(N)=1011:X(N)=(X(24)-X(4))/3+X(4)
420 Y(N)=(Y(24)-Y(4))/3+Y(4)
430 Z(N)=(Z(24)-Z(4))/3+Z(4)
440 N=N+1:NOD(N)=1012:X(N)=(X(24)-X(4))*2/3+X(4)
450 Y(N)=(Y(24)-Y(4))*2/3+Y(4)
460 Z(N)=(Z(24)-Z(4))*2/3+Z(4)
470 N=N+1:NOD(N)=1013:X(N)=(X(25)+X(3))/2!
480 Y(N)=(Y(3)+Y(25))/2!
490 Z(N)=(Z(3)+Z(25))/2!
500 NNODE=N
510 FOR I=1 TO NNODE:Z2(I)=(X(I)*X(I)+Y(I)*Y(I))/(4!*258)
520 NEXT I
530 A=-.98755:B=1!:C=8.02254:D=63.35594
```

```
540 A2=-.98484:B2=1!:C2=7.91704:D2=63.30557#
550 FOR I=1 TO NNODE:T=(-D-A*X(I)-B*Y(I)-C*Z(I))/(A*A+B*B+C*C)
560 XP=A*T+X(I):YP=B*T+Y(I):ZP(I)=C*T+Z(I)
570 DIST(I)=SQR((XP-X(I))*(XP-X(I))+(YP-Y(I))*(YP-Y(I))+(ZP(I)-Z(I))*(ZP(I)-Z(I)
))
580 NEXT I
590 FOR I=1 TO NNODE:T2=(-D2-A2*X(I)-B2*Y(I)-C2*Z2(I))/(A2*A2+B2*B2+C2*C2)
600 XP2=A2*T2+X(I):YP2=B2*T2+Y(I):ZP2(I)=C2*T2+Z2(I)
610 DIST2(I)=SQR((XP2-X(I))*(XP2-X(I))+(YP2-Y(I))*(YP2-Y(I))+(ZP2(I)-Z2(I))*(ZP2
(I)-Z2(I)))
620 NEXT I
630 RMS1=0:FOR I=1 TO NNODE:IF NOD(I)>=401 AND NOD(I)<=426 THEN MULT=1 ELSE MULT
=2
640 IF NOD(I)=401 OR NOD(I)=406 THEN MULT=0
650 RMS1=RMS1+MULT*((DIST(I)+DIST2(I)-DELTAZ)*(DIST(I)+DIST2(I)-DELTAZ))
660 REM PRINT NOD(I);MULT
670 NEXT I
680 RMS=SQR(RMS1/(NNODE+6)):IF RMS<RMSMIN THEN RMSMIN=RMS:DELTAZMIN=DELTAZ
690 REM PRINT " NODE       X          Y          Z         DIST       DIST2      DELTA"
700 REM FOR I=1 TO NNODE
710 REM PRINT USING "#### ";NOD(I);
720 REM PRINT USING "####.#### ";X(I);Y(I);Z(I);DIST(I);DIST2(I);DIST(I)+DIST2(I
)-DELTAZ
730 REM NEXT I
740 PRINT "DELTAZ =";DELTAZ;"  RMS ERROR =";RMS
750 PRINT "MIN DELTAZ =";DELTAZMIN;"MIN RMS ERROR =";RMSMIN
760 PRINT "DO YOU WANT HARDCOPY OF THE INFORMATION (Y/N)":INPUT A$
770 IF A$<>"Y" THEN GOTO 870
780 WIDTH "LPT1:",130
790 LPRINT "DELTAZ =";DELTAZ
800 LPRINT "RMS ERROR =";RMS
810 LPRINT CHR$(27);"Q";
820 LPRINT " NODE       X          Y          Z          ZP         Z2         ZP2
 DIST       DIST2       DELTA"
830 FOR I=1 TO NNODE:LPRINT USING "####  ";NOD(I);
840 LPRINT USING "####.#### ";X(I);Y(I);Z(I);ZP(I);Z2(I);ZP2(I);DIST(I);DIST2(I)
;DIST(I)+DIST2(I)-DELTAZ
850 NEXT I
860 LPRINT CHR$(12)
870 INPUT "ENTER NEW VALUE FOR DELTAZ ",DELTAZ
880 GOTO 630
```

ORIGINAL PAGE IS
OF POOR QUALITY

Standard Bibliographic Page

1. Report No.	2. Government Accession No.	3. Recipient's Catalog No.
NASA CR-178228		

4. Title and Subtitle	5. Report Date
The Integration of a Mesh Reflector to a 15-ft Box Truss Structure, Task 3 -- Box Truss Analysis and Technology Development	March 1987
	6. Performing Organization Code
7. Author(s)	8. Performing Organization Report No.
E.E. Bachtell, W.F. Thiemet, and G. Morosow	MCR-86-669
9. Performing Organization Name and Address	10. Work Unit No.
Martin Marietta Corporation Denver Aerospace P.O. Box 179 Denver, Colorado 80201	506-49-21-01
	11. Contract or Grant No.
	NAS1-17551
12. Sponsoring Agency Name and Address	13. Type of Report and Period Covered
National Aeronautics and Space Administration Wahshington, DC 20546	Contractor Report
	14. Sponsoring Agency Code

15. Supplementary Notes

Langley technical monitors: U.M. Lovelace and J.W. Goslee
Final Report -- Task 3

16. Abstract

In order to demonstrate the design and integration of a reflective mesh surface to a deployable box truss structure, reflective mesh was installed on a 15-ft prototype box truss cube. The resulting configuration is a off-set fed 15-ft diameter reflector with an F/D of 1.5. The resulting surface accuracy was 1/18 of a wavelength at 10 GHz. The specific features demonstrated included:

1) Sewing seams in reflective mesh;
2) Stretching mesh to a desired preload;
3) Installation of a tensioned tie cord support system;
4) Setting and verificlation of a reflective surface; and
5) Repeatability of the reflector surface

17. Key Words (Suggested by Authors(s))	18. Distribution Statement
Large Space Structures Antennas Radiometers Spacecraft	Unclassified - Unlimited Subject Category 18

19. Security Classif.(of this report)	20. Security Classif.(of this page)	21. No. of Pages	22. Price
Unclassified	Unclassified	73	A04

For sale by the National Technical Information Service, Springfield, Virginia 22161